DEPARTMENT OF GEOLOGY AND GEOPHYSICS

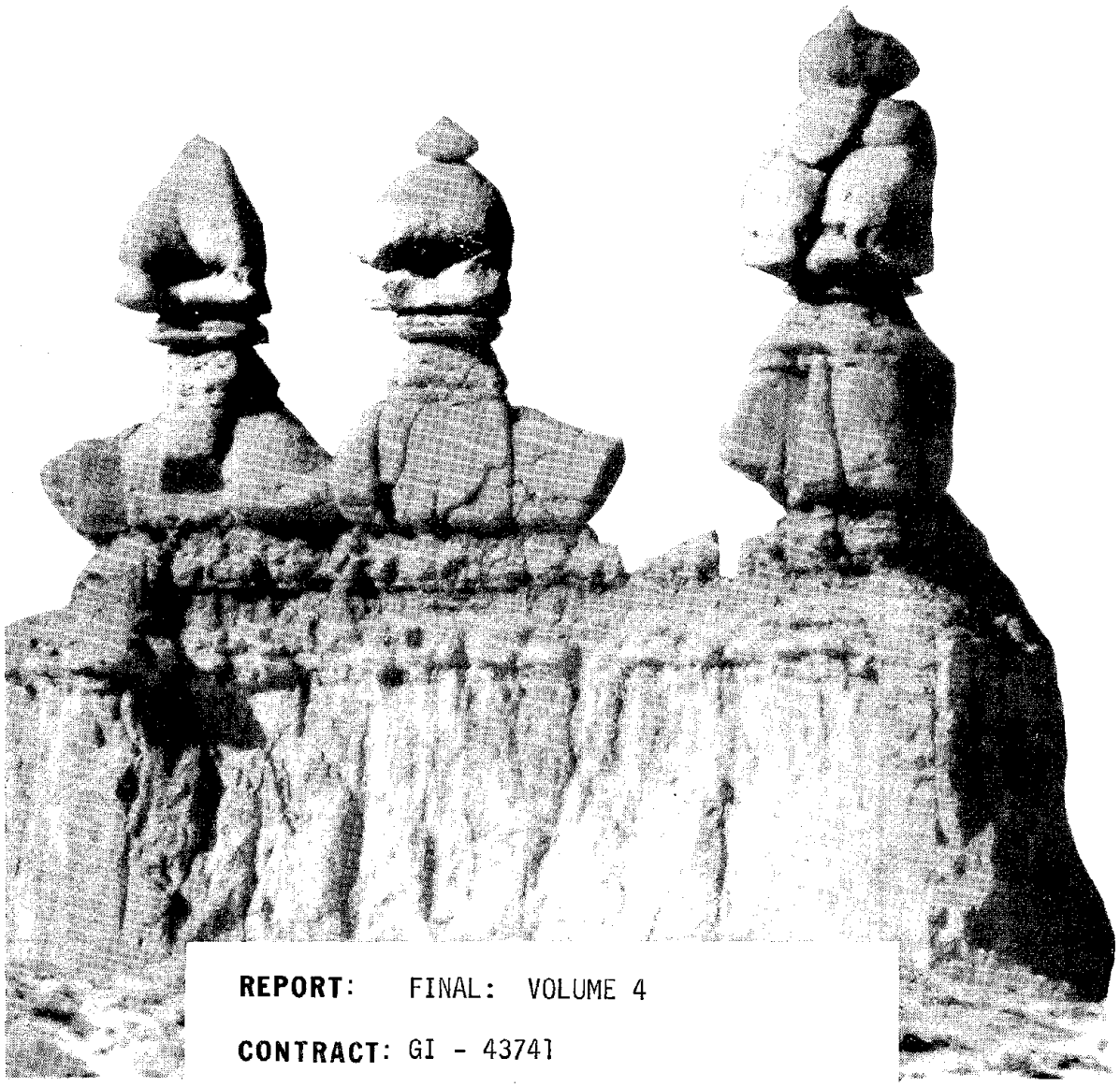

REPORT: FINAL: VOLUME 4

CONTRACT: GI - 43741

AGENCY: NATIONAL SCIENCE FOUNDATION

TITLE: EARTHQUAKE SURVEYS OF THE ROOSEVELT HOT SPRINGS AND THE COVE FORT AREAS, UTAH

AUTHORS: T. L. Olson, R. B. Smith

DATE: October, 1976

UNIVERSITY OF UTAH SALT LAKE CITY, UTAH 84112

BIBLIOGRAPHIC DATA SHEET	1. Report No. NSF/RA-760752	2.	3. Recipient's Accession No.
4. Title and Subtitle Earthquake Surveys of the Roosevelt Hot Springs and the Cove Fort Areas, Utah, Final Report, Volume 4			5. Report Date October 1976 6.
7. Author(s) T.L. Olson, R.B. Smith			8. Performing Organization Rept. No.
9. Performing Organization Name and Address University of Utah Department of Geology and Geophysics Salt Lake City, Utah 84112			10. Project/Task/Work Unit No. 11. Contract/Grant No. AER7401043 GI43741
12. Sponsoring Organization Name and Address Research Applied to National Needs (RANN) National Science Foundation Washington, D.C. 20550			13. Type of Report & Period Covered 14.

15. Supplementary Notes

16. Abstracts

Forty-nine days of earthquake monitoring around the Roosevelt Hot Springs KGRA during 1974 and 1975 indicates little earthquake activity and no correlation with the Hot Springs area. Marked earthquake activity, however, was located 25 km east within the Cove Fort-Sulphurdale KGRA. A total of 163 earthquakes were located from the two surveys. Focal depths for the Cove Fort area were shallow with 75% of the activity less than 5 km in depth. The maximum calculated depth was 16 km. Composite fault plane solutions in the Cove Fort area showed normal faulting with generally east-west trending T-axes. A high b-value of 1.27 and a statistical analysis using the Kolomogorov model of event occurrence imply swarm-like activity near Cove Fort. Consistently positive P-wave residuals of up to 0.10 sec and detectable S-wave attenuation of ray paths across the Mineral Range are suggestive of the possibility of an upper-crustal zone of high attentuation that is perhaps related to the source of heat of the Roosevelt Hot Springs KGRA.

17. Key Words and Document Analysis. 17a. Descriptors

Earthquakes
Surveys
Heat transfer
Geological faults
Soil dynamics
Fluid flow

17b. Identifiers/Open-Ended Terms

Roosevelt Hot Springs KGRA
Cove Fort-Sulphurdale KGRA

17c. COSATI Field/Group

18. Availability Statement	19. Security Class (This Report)	21. No. of Pages
NTIS	UNCLASSIFIED	94
	20. Security Class (This Page) UNCLASSIFIED	22. Price PC A05 / MF A01

EARTHQUAKE SURVEYS OF THE ROOSEVELT HOT SPRINGS AND THE COVE FORT AREAS, UTAH

by

Ted L. Olson and R. B. Smith

PREFACE

The attached report was submitted by T. L. Olson in partial fulfillment of the requirements for the degree of Master of Science in Geophysics, Department of Geology and Geophysics at the University of Utah. The work was performed under the direction of Dr. R. B. Smith.

ACKNOWLEDGMENTS

The author wishes to express his appreciation to Robert B. Smith for his guidance and direction through all facets of this project. William T. Parry and Kenneth L. Cook reviewed the manuscript and made helpful suggestions. Funding was provided for this research by the National Science Foundation Grant GI-43741 to the University of Utah entitled "Geothermal Exploration Systems and their Applications in Utah." Invaluable field assistance was provided from R. D. Armstrong, J. P. Bailey, J. R. Pelton and T. R. Williams. Their assistance is gratefully acknowledged. W. D. Richins also lended support for help in the processing of the data. D. D. Blackwell of Southern Methodist University loaned five portable seismographs used for the 1975 field survey.

TABLE OF CONTENTS

Table of Contents
(continued)

ILLUSTRATIONS

Illustrations
Continued

LIST OF TABLES

ABSTRACT

Forty-nine days of earthquake monitoring around the Roosevelt Hot Springs KGRA during 1974 and 1975 indicates little earthquake activity and no correlation with the hot springs area. Marked earthquake activity, however, was located 25 km east within the Cove Fort-Sulphurdale KGRA. A total of 163 earthquakes were located from the two surveys. Focal depths for the Cove Fort area were shallow with 75% of the activity less than 5 km in depth. The maximum calculated depth was 16 km. Composite fault plane solutions in the Cove Fort area showed normal faulting with generally east-west trending T-axes. A high b-value of 1.27 and a statistical analyses using the Kolomogorov model of event occurrence imply swarm-like activity near Cove Fort. Consistently positive P-wave residuals of up to 0.10 sec. and detectable S-wave attenuation of ray paths across the Mineral Range are suggestive of the possibility of an upper-crustal zone of high attenuation that is perhaps related to the source of heat of the Roosevelt Hot Springs KGRA.

INTRODUCTION

Many geothermal areas throughout the world exhibit earthquake activity in the form of swarms (Ward, 1972). Detailed epicenters and characteristics of earthquake swarms can provide useful information on stress orientation and the possibility of locating fault zones that could provide underground conduits for geothermal fluids. Furthermore, potential earthquakes and related hazards which may influence a geothermal reservoir can be better understood from a detailed assessment of local earthquake activity. It was hoped that an earthquake survey of the Roosevelt Hot Springs and Cove Fort areas of southwestern Utah (Figure 1) could provide information about the geothermal potential of this area and the relationship between the earthquakes and the local tectonic patterns.

Many of the geothermal fields currently being developed are coincident with Quaternary volcanism (McNitt, 1965) that in many cases is characterized by swarm-like activity (Mogi, 1963; Sykes, 1970). Ward (1972) has suggested that the geothermal reservoirs associated with such volcanism can be located by the use of microearthquake monitoring. In particular some geothermal areas, such as The Geysers, California (Lange and Westphal, 1969), Iceland (Ward and Bjornson, 1971), and the Imperial Valley in California (Brune and Allen, 1967) have shown correlations with microearthquake activity. In the intermountain region, Smith and Sbar (1974) found five

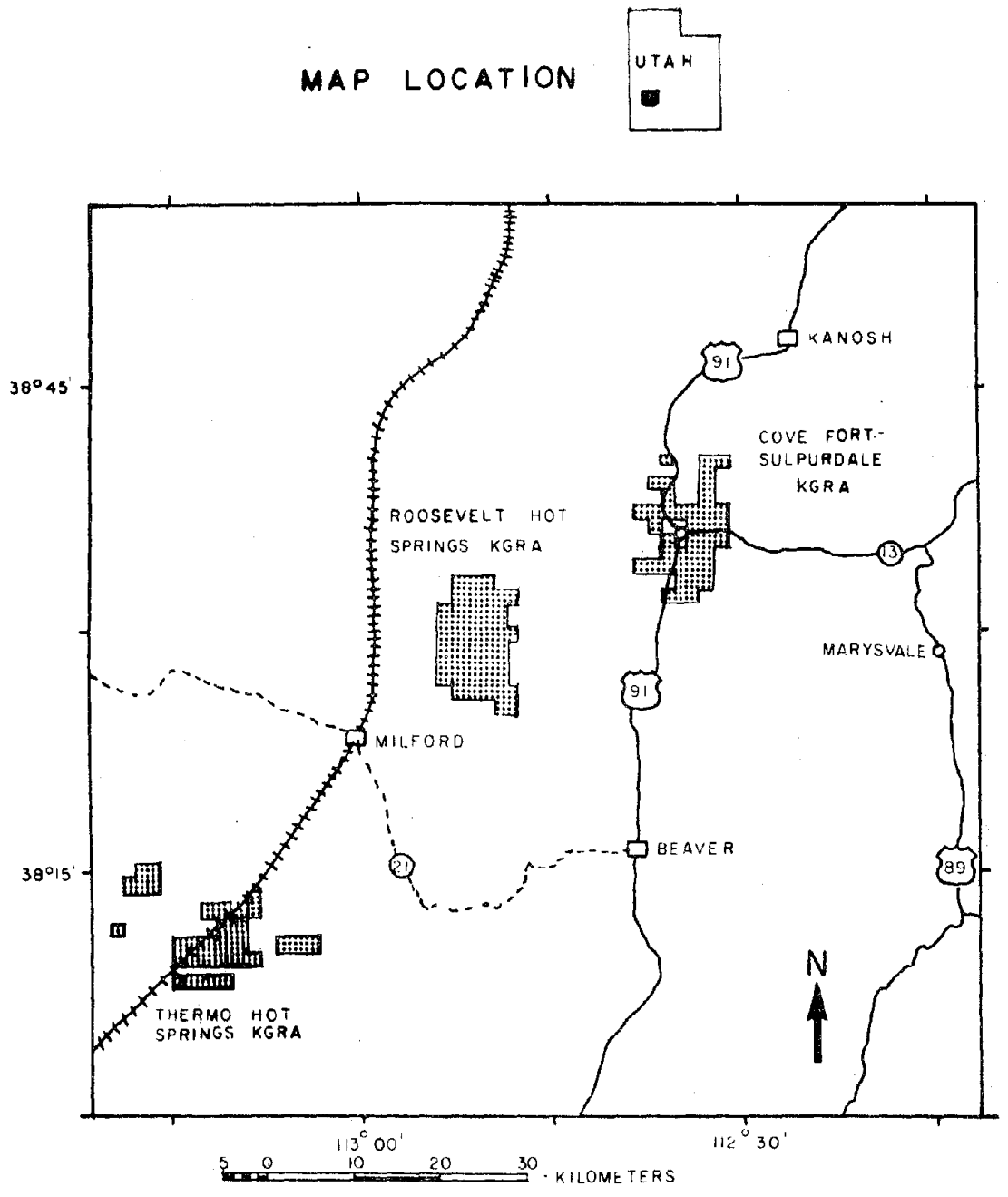

Figure 1
Location of surveyed area.

distinctive earthquake swarm areas coincident with geothermal or volcanic features. Also, the hottest geyser basins in Yellowstone Park were shown by Trimble and Smith (1975) to have prominent swarm occurrences, but they showed a diminution of activity directly within the Yellowstone caldera.

The Roosevelt Hot Springs and the Cove Fort-Sulphurdale areas of southwestern Utah (Figure 1) were surveyed for earthquake activity from September 4, 1974 to September 24, 1974 and from June 11, 1975 to July 8, 1975. The locality surveyed has two known geothermal resource areas abbreviated KGRA (Figure 1): The Roosevelt Hot Springs KGRA, 19 km northeast of Milford, Utah and the Cove Fort-Sulphurdale KGRA, 32 km north of Beaver, Utah. This survey reported here is one part of several geothermal research efforts applied to geothermal exploration methods by the University of Utah.

Although the U. S. Geological Survey has classified three parts of southwestern Utah (Figure 1) as known geothermal resource areas, previous to this survey few geophysical investigations had been made in these areas. The most extensive work was carried out by the University of Utah during the summers of 1974 and 1975. Research and exploration carried out by the University include geologic mapping, resistivity, gravity, magnetics, geochemistry evaluation, electromagnetic sounding and heat flow as well as the survey reported here.

As part of a commercial exploration effort, Union Oil Company and Phillips Petroleum Company have performed reconnaissance surveys of induced polarization, hydrochemistry, gravity, and magnetics. On the

basis of favorable results from these investigations, the two companies have leased many tracts of land in the area. More noteworthy, Phillips Petroleum Company has drilled several wells near the Roosevelt Hot Springs, one of which has yielded steam from a reservoir in excess of 200°C (Berge and others, 1975) and may be of commercial value by 1980 (Crosby, personal communication, 1975).

GEOLOGICAL AND GEOPHYSICAL BACKGROUND

The Milford-Cove Fort area of southwestern Utah lies at the eastern margin of the Basin-Range province at the transition into the Colorado Plateau. The surveyed area lies in an east-west zone of thick Tertiary, silicious volcanics that extend from the Tushar Mountains (Plate 2) across the grain of the north-south Basin and Range faulting and into southern Nevada. Hot springs and hydrothermal alteration are closely associated with this zone (Heylmun, 1966).

The north-trending Mineral Range (Plate 1) is the dominant topographic feature of the surveyed area and is bounded by two alluvial valleys. The west flank of the range is bounded by the north extremity of the Escalante Desert or Milford Valley (Plate 1) and the east flank is bounded by the Beaver Valley (Plate 1).

Milford-Roosevelt Area

Most of the Mineral Range is composed of Tertiary granite with Precambrian(?) metamorphics and Tertiary volcanics along the west flank and some Paleozoic quartzites at the north end. Rhyolite domes and obsidian flows extrude and overlie portions of the granite. Two ages of the volcanic activity obtained from K-Ar dates by Mehnert (1975) for the Mineral Range indicate 0.77 ± 0.08 m.y. for the older volcanics and 0.42 ± 0.07 m.y. for the younger.

Midway along the west flank of the Mineral Range evidence of hydrothermal alteration is apparent near the Roosevelt Hot Springs

(W. T. Parry, personal communication) and along the Dome Fault (Plate 1, Peterson, 1975), which trends north-south. An opal deposit has been offset by the Dome Fault and is probably an expression of earlier hot spring activity (Peterson, 1975).

Gravity surveys were conducted in the fall of 1974 and the summer of 1975 in the Roosevelt Hot Springs area by the University of Utah (Crebs, 1976; Thangsuphanich, 1976) and indicate the Dome Fault to be just one of several northward-trending normal faults in the immediate area. Previous to these latest gravity surveys this fault zone was only inferred. A density contrast of 0.5g/cc between the alluvium and bedrock implies a fault with a throw of 600 m, 8 km south of the Roosevelt Hot Springs and three faults with a maximum throw of 100 m at the north end of the Mineral Range. A digitally filtered map of the Bouguer gravity data indicates a northward-trending, elongated gravity low of at least 3 mgal closure over three volcanic domes; South Twin Flat Mountain, North Twin Flat Mountain, and Bearskin Mountain (Plate 1) in the Mineral Range (Crebs, 1976). Mass deficiency calculations for this anomaly (Crebs, 1976) imply the presence of a low density zone which could be caused by a zone of partial melt.

Cove Fort-Sulphurdale Area

The rugged Tushar Mountains (Plate 2) southeast of Cove Fort were the scene of intense Tertiary intrusive and extrusive igneous activity. Early Quaternary volcanic activity was extensive, but became intermittent by early Pleistocene time (Willard and Callaghan, 1962). The volcanic rocks of the area are now displaced by normal

faults of probable Pleistocene age, and the present major structural blocks are the principal results of normal faulting.

Sulphur deposits, fluorspar, and other base metals associated with the Tushar intrusives are present along the west flank of the mountains and also occur northward in the southern Pavant Range (Plate 2). Lee (1906) implied the definite association of these sulphur deposits as well as the sulphur deposits at Sulphurdale (Plate 2), with the north-trending zone of intense faulting along the west flanks of the Tushar Mountains and the Pavant Range. Hot springs of low pH and a water well with temperatures of 91^{o}C in eastern Dog Valley (Crosby, 1959; Plate 2) are also associated with this same zone described by Lee (1906). A regional gravity survey conducted by Sontag (1965) indicates the fault zone (Figure 15) parallels U. S. Highway 91 (Figure 1) and extends from Beaver (Figure 1) northward beyond Cove Fort.

The area west of Cove Fort is covered by a variety of Cenozoic and Paleozoic sedimentary rocks, however, about 25% of the surface rock are extrusives consisting of Tertiary rhyolites and andesites, as well as Quaternary basalts, and vitrophyre exposures (Zimmerman, 1961). Minor north-trending normal faults cut through the extrusives and Crosby (1973) and E. Clark (personal communication, 1975) have stated that strike-slip components are detectable.

A regionally significant structural zone occurs between the Pavant Range and the north end of the Beaver Lake Mountains (Plate 1). Because of a westward offset of major north-trending thrusts apparent in the two ranges, Crosby (1973) has described the areas as the "Black Rock offset". East-west trends on the Utah gravity map (Cook et al.,

1975), and the Utah aeromagnetic map (Shuey, 1975), along with a steep gravity gradient reported by Eaton (1975) are coincident with this offset zone.

In general the surveyed area has a history of volcanic activity and complex structure (Crosby, 1973).

HISTORICAL SEISMICITY

The Intermountain Seismic Belt is a zone of pronounced earthquake activity that extends north from Arizona through Utah, eastern Idaho and into western Montana (Figure 2). Two secondary easterly trending seismic zones are recognized in the intermountain region (Smith and Sbar, 1974). The Idaho seismic zone extends westward north of the Snake River Plain. The other zone extends from southwestern Utah through southern Nevada and joins the north-trending Nevada seismic zone (Smith and Sbar, 1974). The second zone intersects the Intermountain Seismic Belt in an area extending northward from Cedar City, Utah (Figure 15) into the surveyed area. Seismic activity of this east-trending zone is coincident with Tertiary age rhyolites and an east-west zone of calderas, however, it is not aligned with the regional north-south tectonic grain associated with the Basin-Range normal faulting.

The Sevier and Tushar fault zones (Figure 15), which are 40 km east of the surveyed area, have been found to be one of the most seismic active areas of Utah (Cook and Smith, 1967; Sbar and others, 1972). The historic seismic activity of the Roosevelt and Cove Fort areas of southwestern Utah shows a relatively low level when compared to this area. However, five shocks with maximum estimated Mercalli intensity VI occurred in the Beaver Lake Mountains (Plate 1), 18 km northwest of Milford in 1908 (Williams and Tapper, 1953). And, as

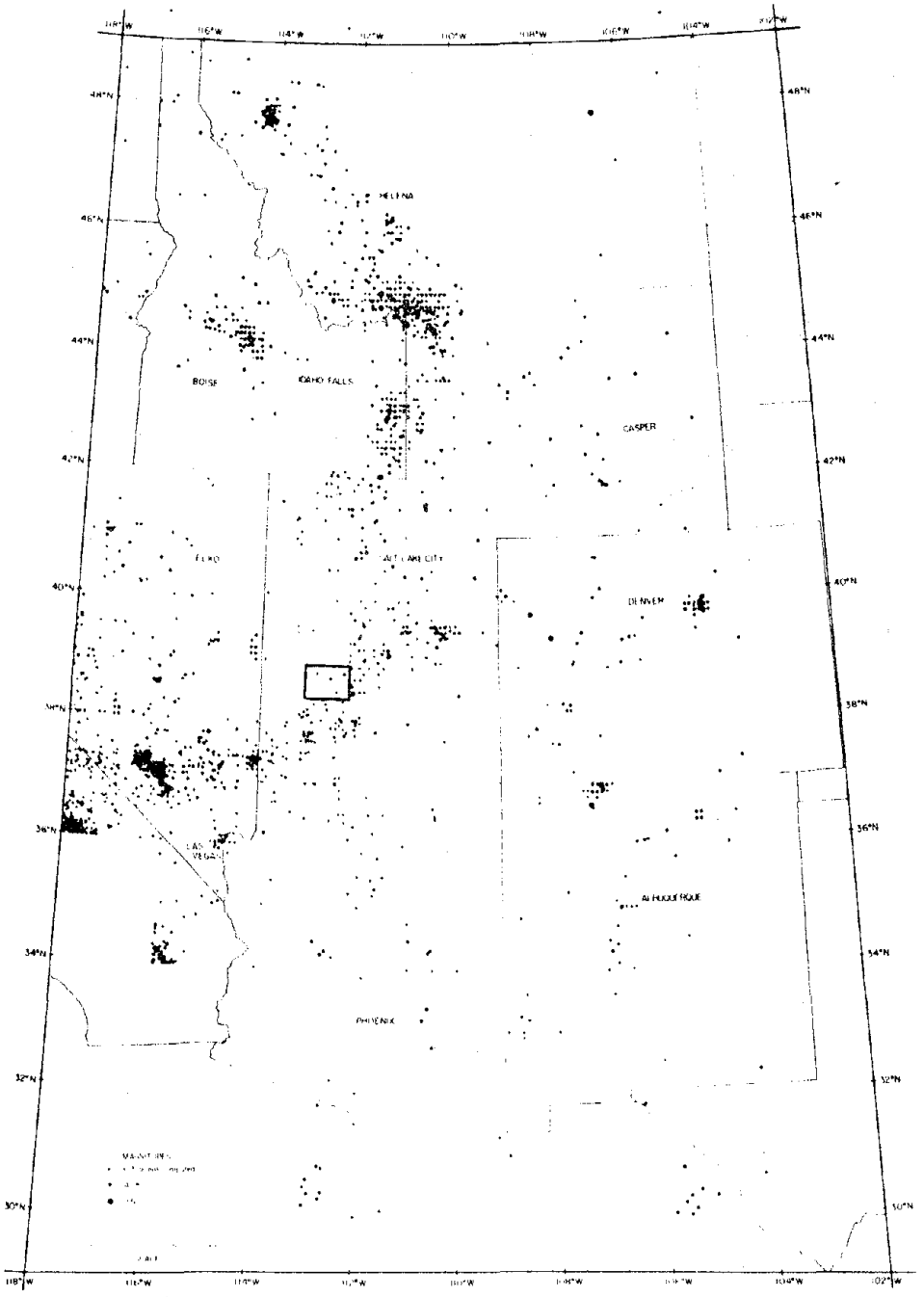

Figure 2
Index map and regional seismicity.
Regional seismicity taken from Smith (1975).

late as 1966, an earthquake of magnitude 4.9 was located near the Milford area (NOAA Historical File of Earthquakes).

The north end of the Hurricane Fault Zone (Figure 15) has experienced sporatic earthquake activity with intensities as large as V in both the Beaver and Cove Fort areas in past years (Williams and Tapper, 1953; Cook and Smith, 1967). As recently as September 10, 1975, the University of Utah seismograph network located a M_L 2.9 earthquake 6 km northwest of Cove Fort (W. D. Richins, personal communication). Based upon 117 reported events (Cook and Smith, 1967) three times as much activity has been reported in the Marysvale area (Figure 1) 40 km east. This documents the fact that although sporatic activity has occurred in the surveyed area, a much higher rate of activity is associated with the major fault zones to the east (Figure 15).

DATA COLLECTION AND REDUCTION

The survey reported on here was made during two different periods. The first, a reconnaissance survey, lasted 21 days in September 1974 and the second, a detailed survey, lasted 28 days during June and July of 1975.

The data for the 1974 survey were recorded with six Sprengnether high-gain portable seismographs. Data were recorded on smoked paper records with five instruments recording at a rate of 30 mm/min, and one instrument at 60 mm/min. The 1975 portion of the survey was made using eleven instruments. All records for the 1975 survey were recorded at 60 mm/min.

Timing for both surveys was provided from internal crystal clocks, accurate to 1 part in 10^8, and each clock was calibrated at least every other day against radio station WWV. The displacement magnifications of the instruments ranged from 0.35×10^6 to 1.6×10^7 times at 10 hz. All seismometers were operated continuously in the vertical mode.

The 1974 survey had a twofold purpose. First, detailed coverage of the Roosevelt Hot Springs area was provided with an inner-tripartite array with 20 km legs. Secondly, a 45 km leg tripartite array was designed to give broad regional coverage. The outer array was centered over the inner array to give good multiple coverage and to also determine the extent of any activity detected from the

Roosevelt Hot Springs area (Figure 3).

The 1975 survey was designed to investigate areas of activity located in the earlier 1974 reconnaissance survey. Detailed coverage was obtained around the Cove Fort area and continued monitoring of the Roosevelt Hot Springs area was also maintained (Figure 3).

Although cultural noise was minimal, without exception all station locations were located at least 400 meters away from secondary roads used for access. Latitude and longitude locations for each station site are indicated in appendix B.

With the aid of microscopes, initial motions and times of P-arrivals to ±0.1 sec were picked. S-arrivals, where apparent, were also picked to the same degree of accuracy.

Velocity Models

The initial velocity model (Figure 4a) was taken from the Delta-West refraction profile (Mueller and Landisman, 1971), which is 50 km north-northwest of the Roosevelt Hot Springs KGRA. S-wave velocities corresponding to this velocity model were obtained assuming a Poisson's ratio of 0.25. Using both P- and S-wave arrival times, preliminary hypocenter locations were obtained with the computer program HYPO71 (Lee and Lahr, 1972). A total of 163 earthquakes, ranging in magnitudes from -0.5 to 2.8 were correlated on 3 or more stations and located.

Inversion techniques developed by Michaels (1973) were then performed to more accurately define the velocity model for the Cove Fort area. The generalized inverse method used, performs successive

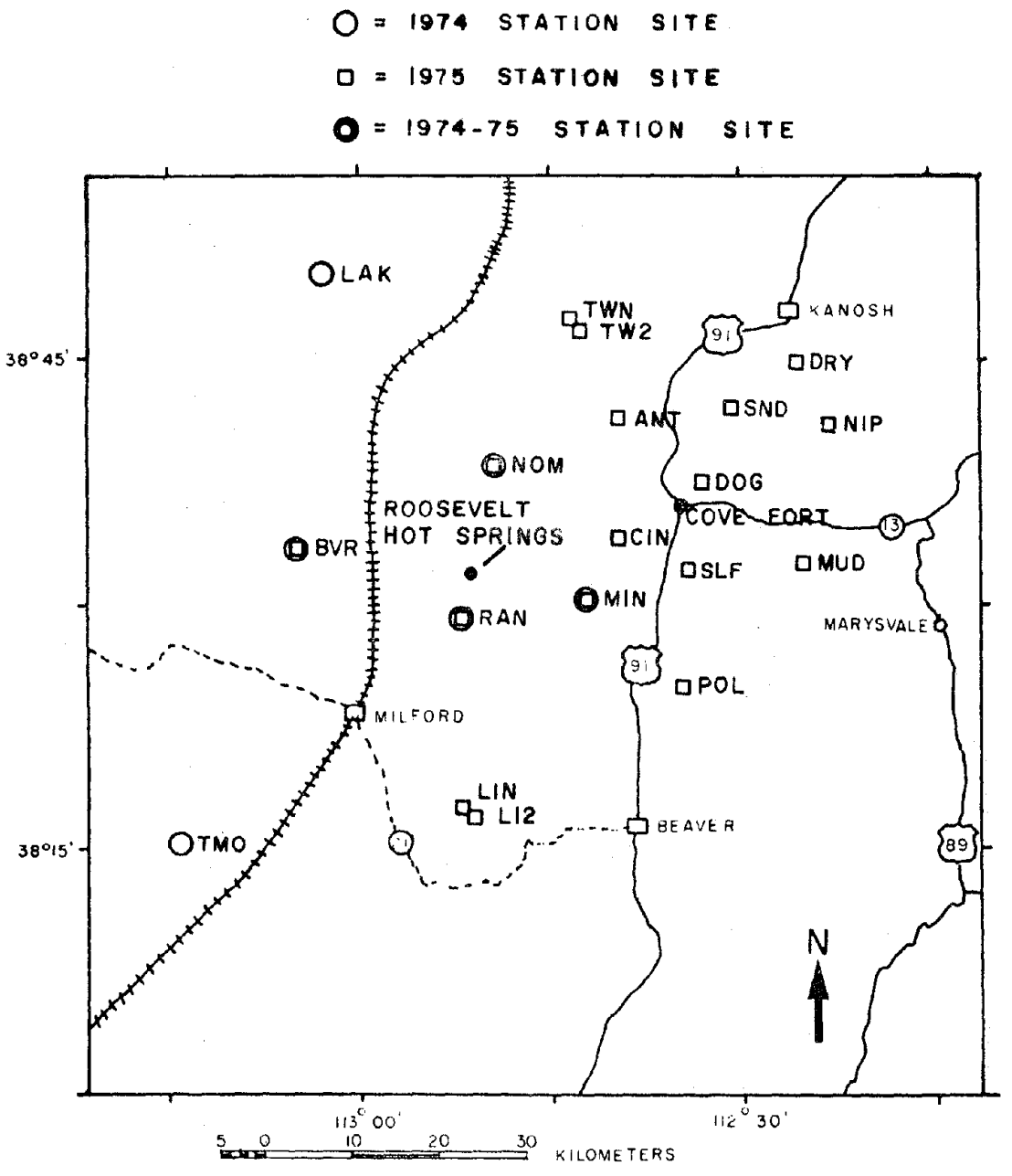

Figure 3
Station locations for 1974-75 surveys.

VELOCITY (km/sec)	DEPTH TO TOP (km)	THICKNESS (km)
3.0	0.0	2.0
5.9	2.0	13.0
6.4	15.0	13.0
7.4	26.0	SEMI-INFINITE

a) The Delta-West profile velocity model.

VELOCITY (km/sec)	DEPTH TO TOP (km)	THICKNESS (km)
3.1	0.0	0.4
5.7	0.4	13.8
6.4	14.3	11.7
7.4	26.0	SEMI-INFINITE

b) Final velocity model with top two layers derived from linear inversion.

FIGURE 4
Velocity models.

iterations on both layer thickness and velocity. A systems matrix involving partial derivatives of travel times with respect to velocities and hypocenter is inverted using a multivariate version of Newton's method. Finally a least-squares technique is employed to minimize the error. Good preliminary hypocenter locations of six earthquakes appearing on the same five stations or five earthquakes on six stations is necessary to apply the method.

Eight sets of data appearing on the same five stations were used from the Cove Fort area. The preliminary hypocenters used had an RMS error less than 0.10 sec and were determined by using the Delta-West velocity model. No inversion could be performed for the deeper layers because of the absence of deep focal depths. The resulting velocity model consists of the two top layers, determined from inversion, and the third layer and semi-infinite half space from the Delta-West velocity model. The final velocity model used is shown in Figure 4b. The earthquake locations were again computed using the program HYPO71, and are listed in appendix A.

The hypocenter accuracy is based on both the statistical measure of the solution (RMS of time residuals) and the nature of the station distribution with respect to the earthquake. A statistical estimate of hypocenter accuracy can be defined with a contoured surface of the least-squares error for P-wave travel time residuals on a plane containing the hypocenter. Such a contoured surface is called a solution space.

Using a program developed by Michaels (1973), solution spaces in X-Y and X-Z planes were computed for several earthquakes at Cove Fort.

Typical solution spaces with elliptical shaped contours for an earthquake located 5 km northeast of Cove Fort (Plate 2) are shown in figure 5. For the 0.1 sec. contour, the earthquake within the array was located to within ±0.7 km in X-Y and to ±2.3 km in focal depth.

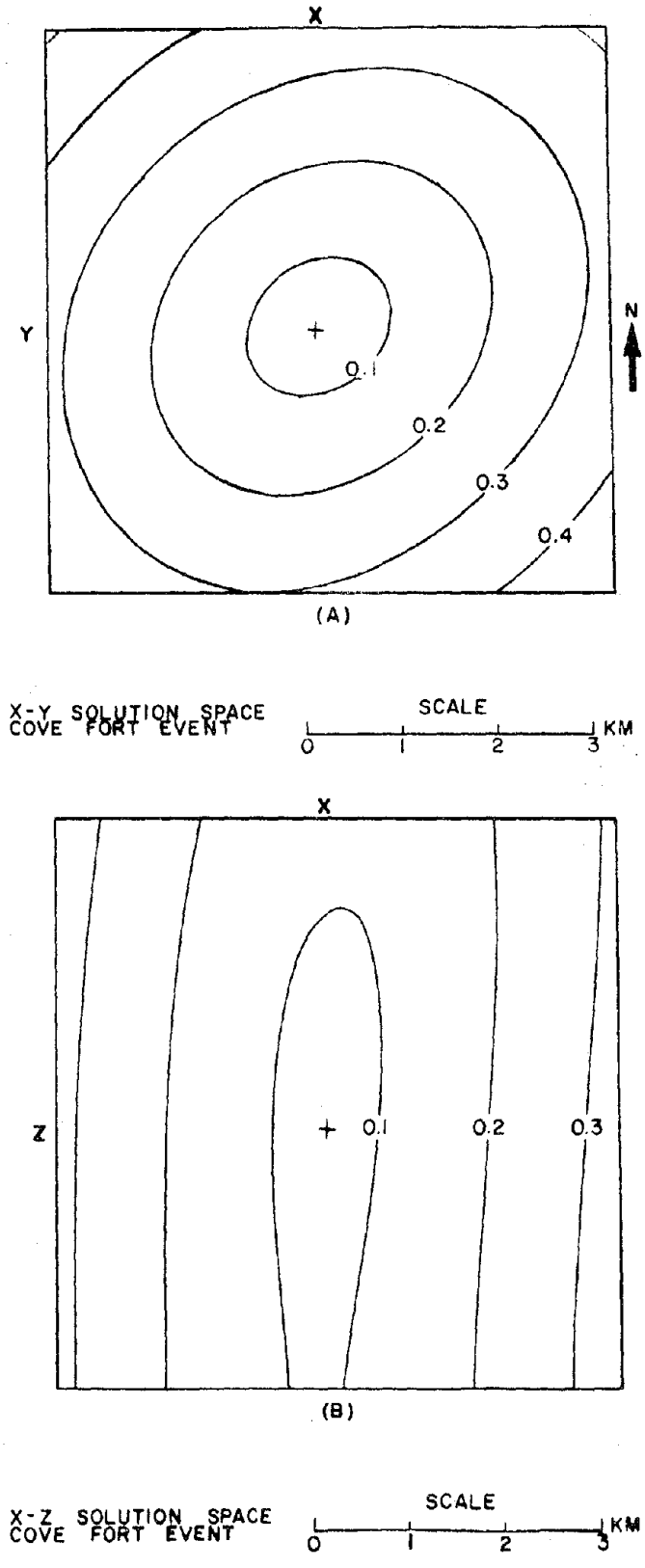

Figure 5
Solution spaces for the Cove Fort area.

CONTEMPORARY SEISMICITY

Plate 1 shows the epicenters from the 1974-75 surveys superimposed on the general geology of the Roosevelt Hot Springs area. Focal depths have been subdivided into three categories: less than 5 km, 5 km to 10 km inclusive, and greater than 10 km. Three predominant characteristics of the earthquake activity can be observed:

1. Several earthquakes are located along a north-south trend northwest of Milford,
2. Six earthquakes are aligned along the west flank of the Mineral Range, perhaps along the Dome fault,
3. The amount of earthquake activity increases rapidly in the northeast portion of the surveyed area, near the Cove Fort KGRA.

The earthquakes northwest of Milford have focal depths ranging from 1.5 km to 13 km. These events occur along the west side of the Milford Valley graben described by Berge et al (1975), presumably along a boundary fault. This graben is filled with 1.7 km of alluvium (Crebs, 1976), and the microearthquake activity suggests that the boundary fault(s) of the graben may still be active.

The earthquakes located along the west flank of the Mineral Range coincide with a north-trending fault zone detected by gravity surveys (Crebs, 1976; Thangsuphanich, 1976). The focal depths for four of these earthquakes were not resolved, but two earthquakes closest to the hot springs had shallow focal depths less than 2 km. A histogram of focal depths showing the shallow extent of the activity in the

Roosevelt area is shown in figure 6.

The increase of earthquake activity from the north edge of the Mineral Range east to Cove Fort occurs in a zone of Quaternary basalt flows. From plate 2 the number of earthquakes continue to increase eastward of this zone. The number of earthquakes west of longitude 112° 45' W (Roosevelt Hot Springs area) is about a fifth as many as those in the Cove Fort area (Plate 2).

Epicenters and general geology for the Cove Fort area are shown on Plate 2. The most prominent characteristic is a large cluster of earthquakes 3 km northeast of Cove Fort in a zone of high earthquake activity extending northward. Cross Section A-A' (Figure 8) strikes N 85° E (Plate 2) and includes all earthquakes in this cluster with resolved focal depths within 2 km on each side of the profile. The attitudes of these hypocenter patterns suggests a north-trending fault dipping about 70° W, with predominantly shallow seismic activity less than 5 km in focal depth. Sontag (1965) indicated a north-trending fault in the area of highest seismic activity northeast of Cove Fort. Crosby (1959) also inferred northeast-trending normal fualting to be present in the same area, but gave no conclusive evidence of the location. Because the epicenters along this fault have epicentral errors less than 1 km, the location of the fault must be just west of Sulphur Peak (Plate 2). For comparison, a map of the epicenters for the Roosevelt Hot Spring and Cove Fort areas is indicated in figure 7.

Cross section B-B' (Figure 8) strikes N 69° W through Dog Valley (Plate 2) and indicates a diffuse pattern of activity with no apparent

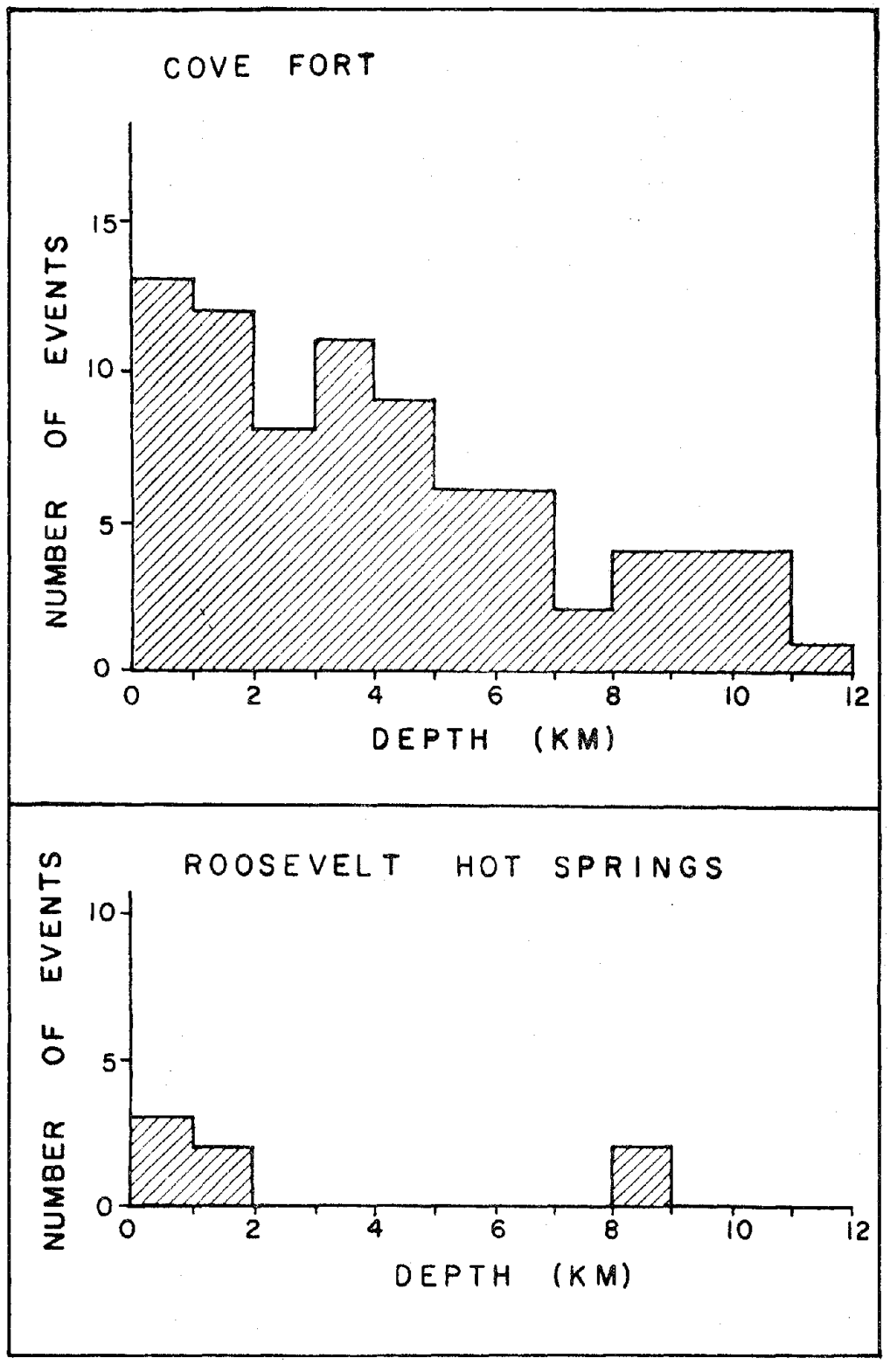

Figure 6
Earthquakes versus focal depth.

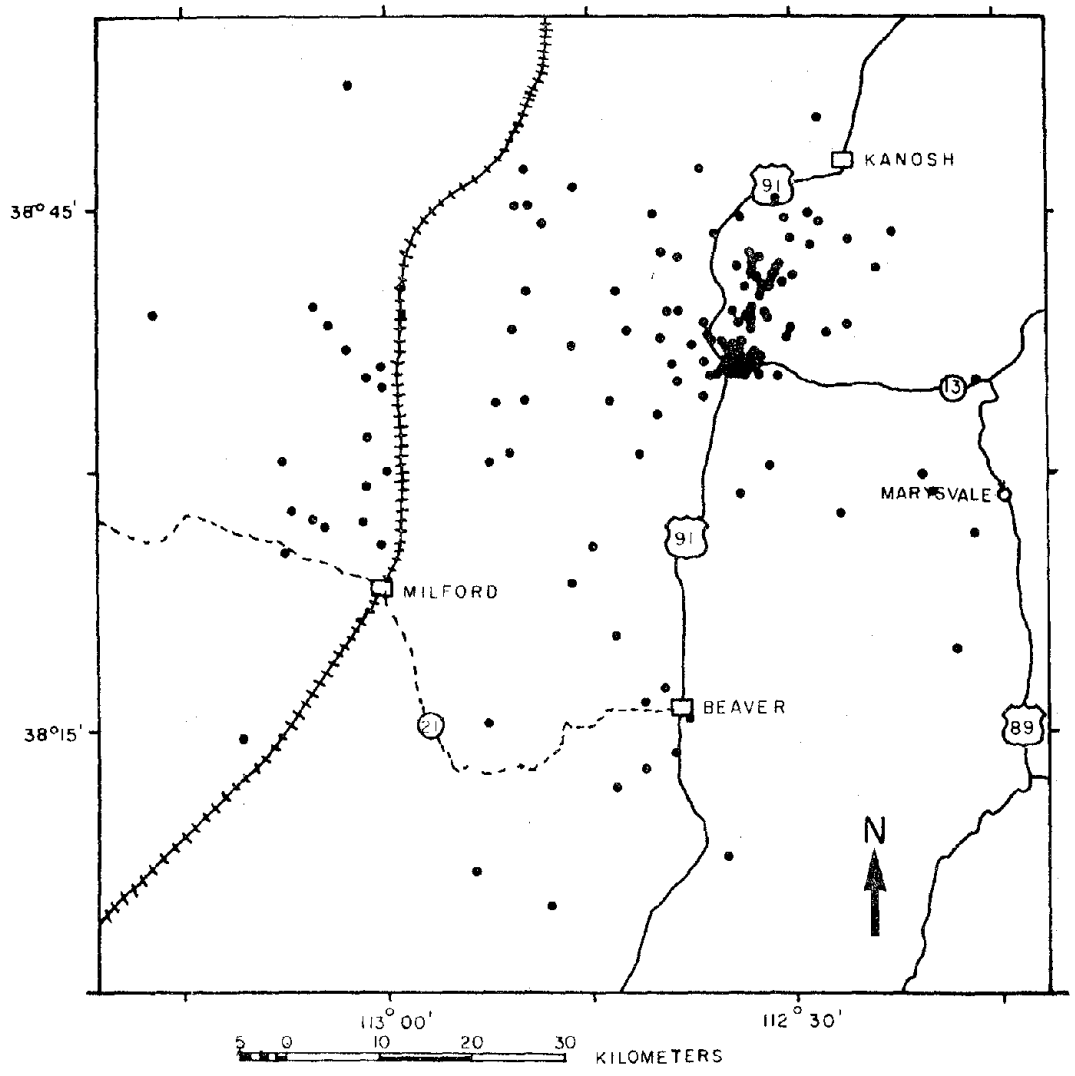

Figure 7
Epicenter map for the Roosevelt Hot Springs
and Cove Fort areas.

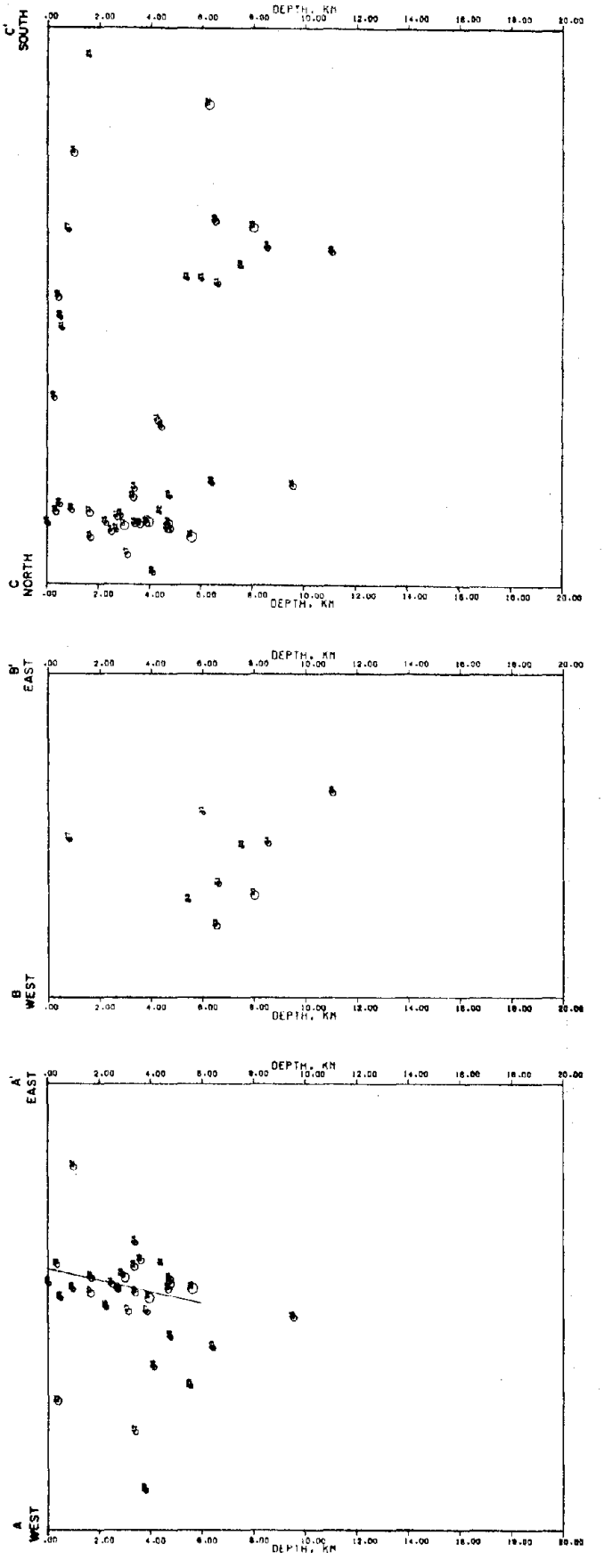

Figure 8
Focal depth cross sections. Horizontal scale same as vertical.

relationship to a single fault plane. All focal depths except one are deeper than 5 km implying that the active zone here is deeper than the area south near Cove Fort. Cross section C-C' (Figure 8) shows the general focal depth variation along the west flank of the southern Pavant Range (Plate 2). In general the activity becomes deeper to the north.

Diffuse epicenter locations extending northward from Dog Valley and westward from Cove Fort do not appear to be associated with a single fault in either locality. Several explanations can be offered for the scatter of the epicenters. A complex fracture zone linked to a single fault could relieve stored strain at a distance away from the mapped surface structure. Another possibility is the presence of transverse faulting (east trending faults in this case) that could still be active. W. D. Brumbaugh (personal communication, 1976) has conducted detailed gravity surveys in the Dog Valley area and indicates minor east-trending faults to be present. If these faults are active, the diffuse pattern in Dog Valley area could very well be attributed to them.

In general, the Cove Fort area is characterized by a high rate of shallow earthquake activity. Figure 6 indicates that 75 percent of the focal depths are less than 5 km. The shallowest earthquakes are clustered together northeast of Cove Fort, while the deeper events (5 to 10 km) are located in the Dog Valley area.

Earthquake Occurrence and Clustering

The number of located events per day for the 1974 and 1975

surveys is plotted in figure 9. The average number of located earthquakes per day is about five.

Perhaps of more interest is the amount of activity measured at individual stations. A total of 405 earthquakes were detected at the Dog Valley station, DOG (Figure 10). During three particular days (June 16, 22, 30, 1975) the Dog Valley station showed clustering of earthquakes lasting only a few hours (Figure 12). No single event stood out as a major shock, but rather, general seismicity gradually increased to a high level and then decreased. These clusters seem to have a swarm-like nature as described by Mogi (1963). The Ranch Canyon station (RAN) which was 6 km from the Roosevelt Hot Springs, however, showed a marked decrease in seismic activity (Figure 11).

S minus P times for the Dog Valley station as well as three other selected stations are indicated in figure 13. The Antelope Valley (ANT) and Dog Valley stations indicate a close proximity to activity, while the Ranch Canyon and North Mineral stations indicate a correlation of 3-5 seconds or about 21-35 km distance from major sources of activity. No stations along the Mineral Range indicated any immediate localization of activity. The RAN station site was nearest to the Roosevelt Hot Springs, but failed to detect any earthquakes which were not detected on other stations.

The data presented here do not entirely agree with the suggestion by Ward (1972), that "large numbers of microearthquakes are often found within, but not outside of geothermal areas". Little activity during our surveys was found to be present in the Roosevelt Hot Springs KGRA. There are several possible explanations of this low

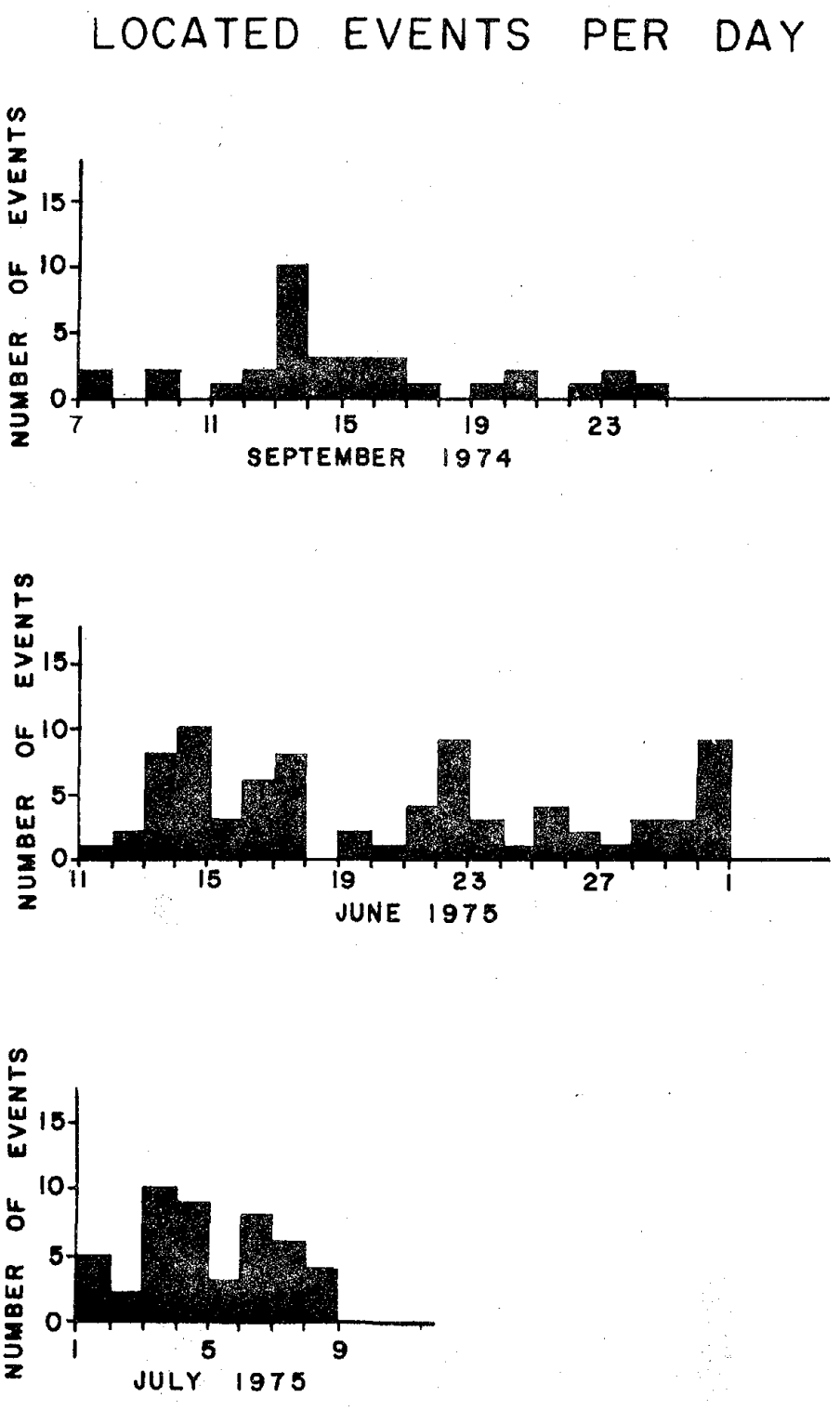

Figure 9
Earthquake histrogram for 1974-75 surveys.

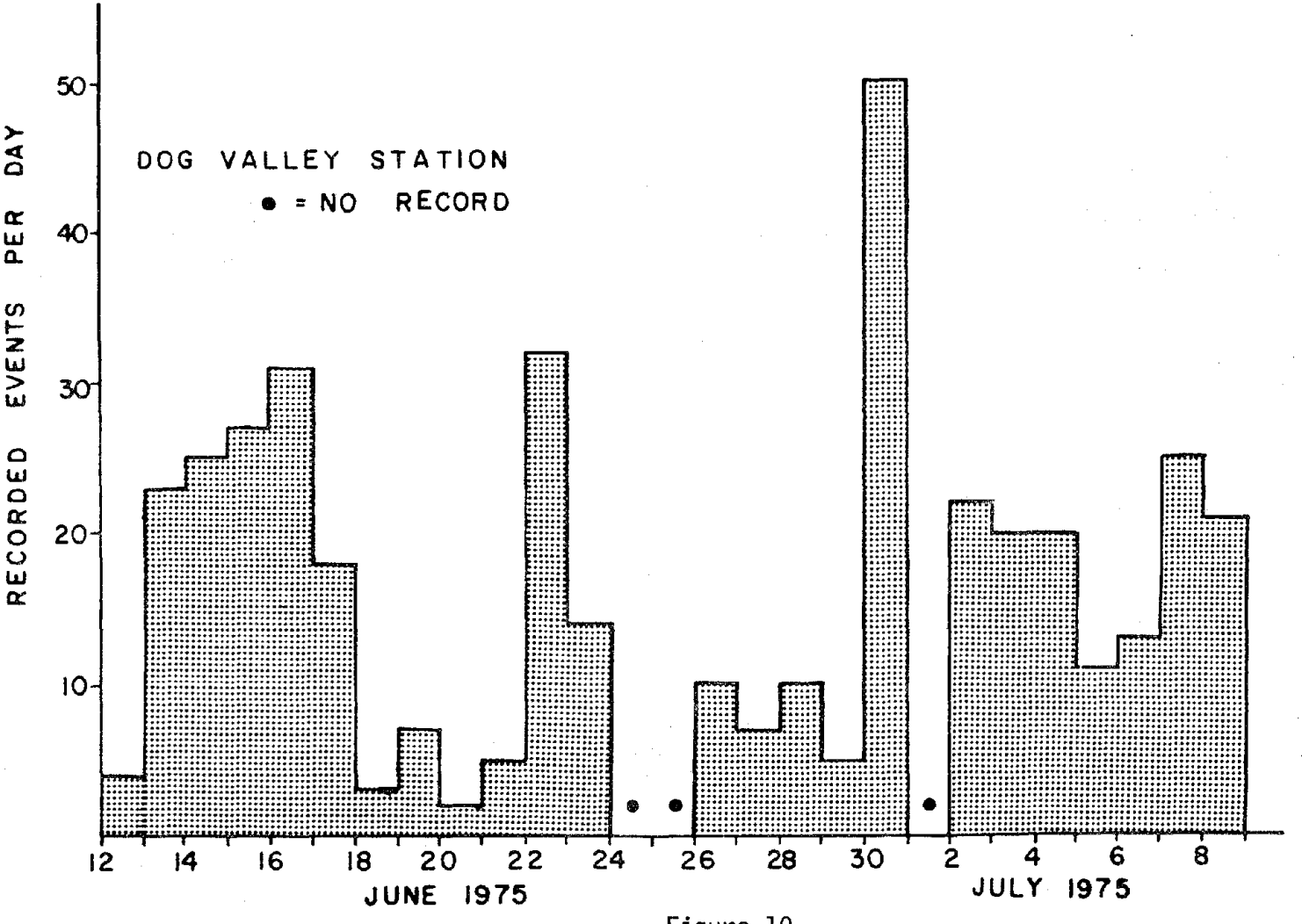

Figure 10
Earthquake histogram for the Dog Valley Station.

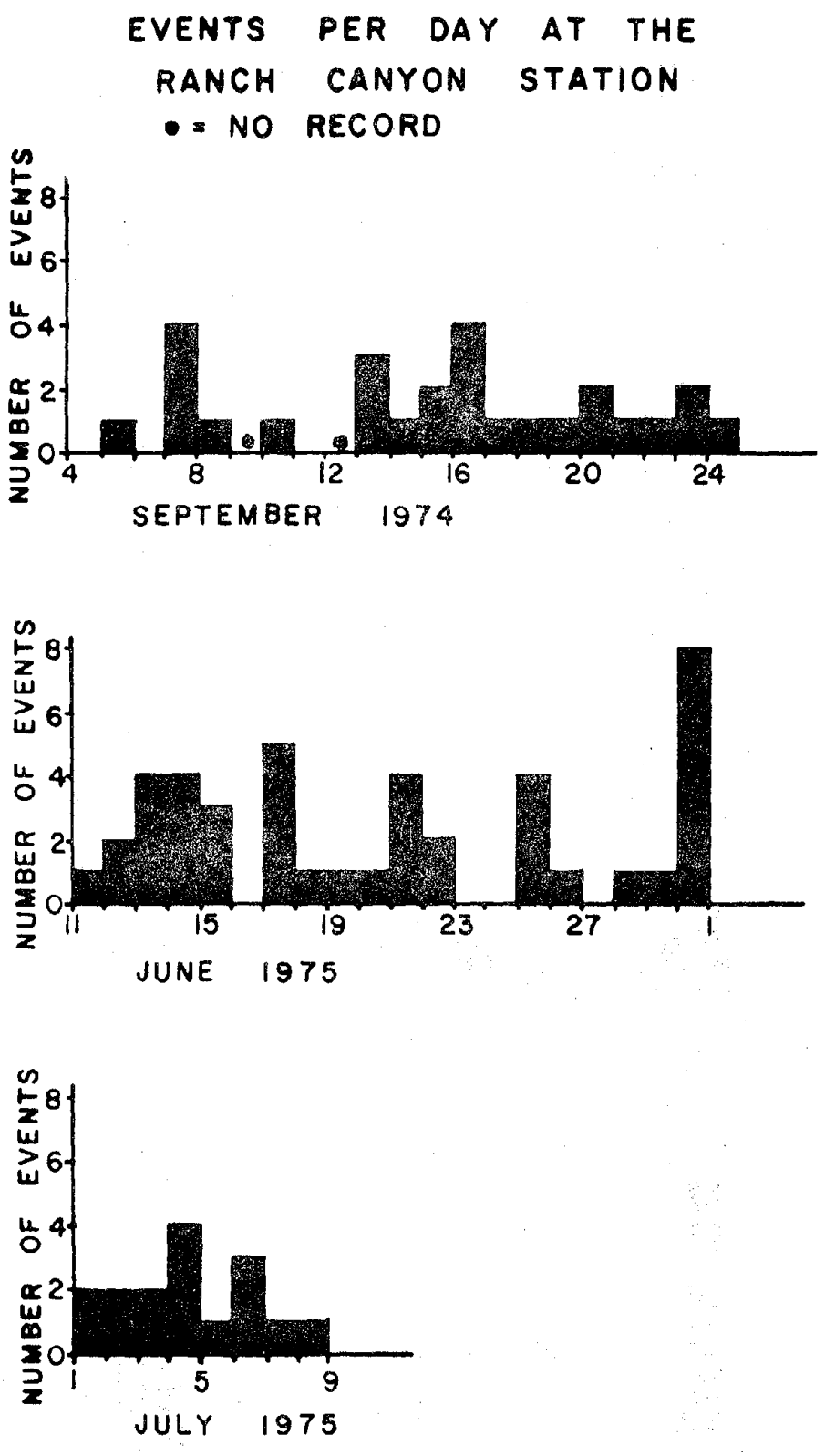

Figure 11
Earthquake histogram for the Ranch Canyon Station.

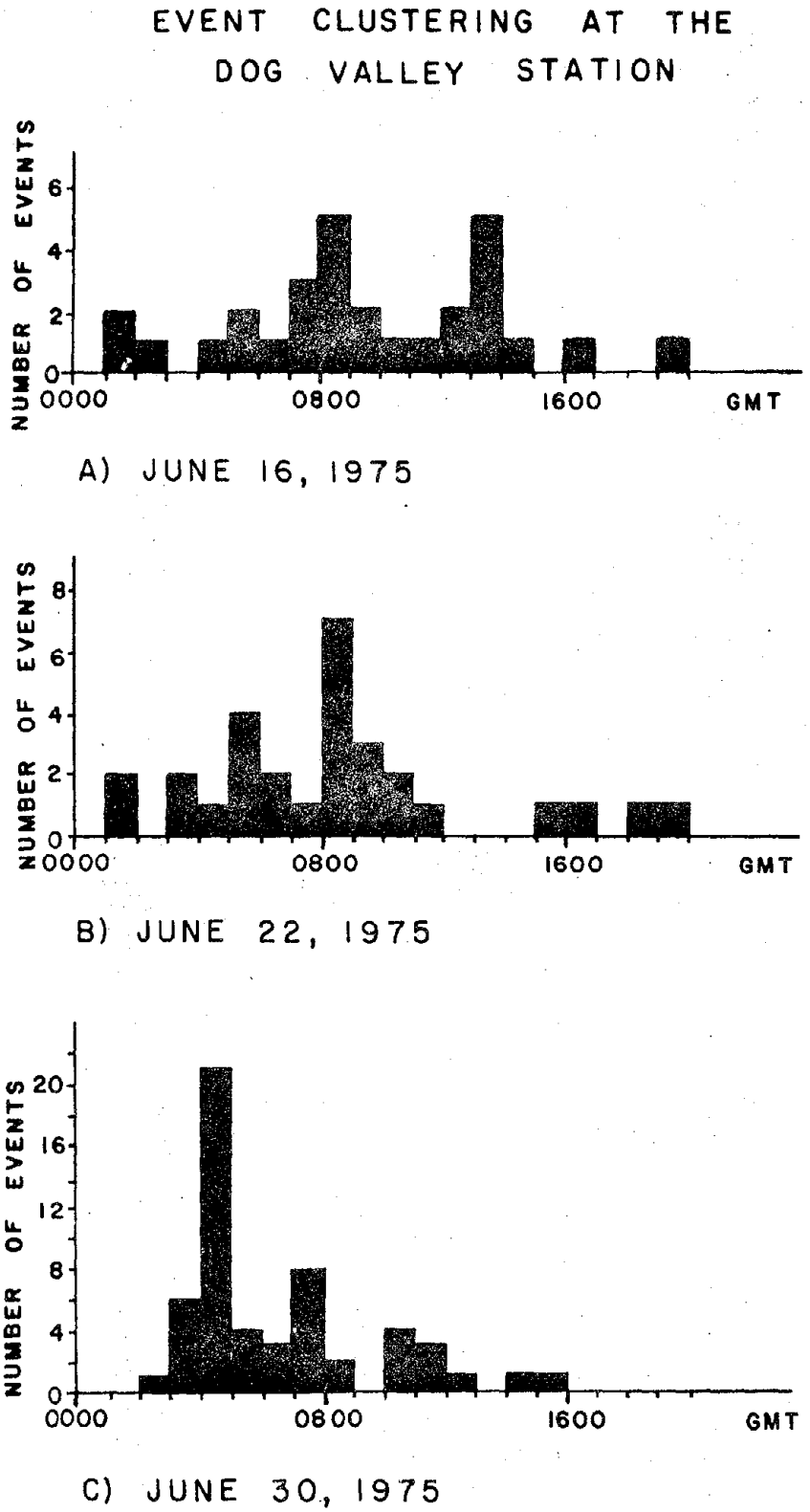

Figure 12
Earthquake clustering for the Dog Valley Station.

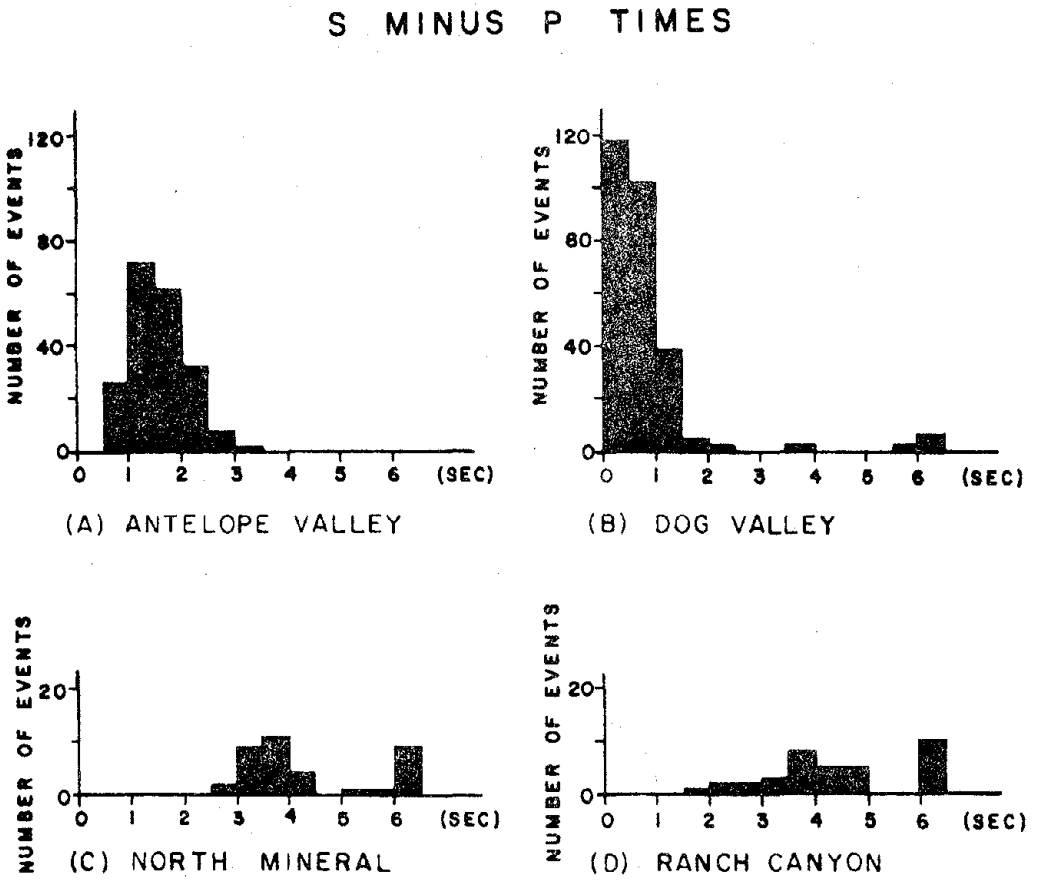

Figure 13
S minus P times for various stations.

rate of activity:

1. The microearthquakes of the Roosevelt area were too small to detect by our network. Our network recorded events as small as magnitude -0.5.

2. The recording periods were made during seismically quiet times suggesting the possibility of episodic activity.

3. The Roosevelt Hot Springs may not be seismically active.

4. High temperatures may produce stable sliding instead of stick-slip movement (Brace and Byerlee, 1970).

5. A zone of partial melt near the surface may not be strong enough to sustain strain accumulation required for stick-slip stress drops.

Steeples and Pitt (1976) have made similar analyses of microearthquake activity in Long Valley, California. An analogous situation was found at the Marysville, Montana heat flow anomaly (Friedline et al., 1976) for which heat flow ranges from 3.2 hfu to 19.5 hfu (Blackwell and Bagg, 1973). Friedline et al. (1976) suggest that the marked absence of seismic activity could be a result of high temperatures of high pore pressure.

Whatever the explanation, the microearthquakes recorded are predominently northeast of the Roosevelt Hot Springs, centered near Cove Fort. It was not possible to distinguish from the small number of earthquakes the attitude of a possible fault zone that could facilitate upward movement of steam or hot water.

Magnitudes and b-values

Magnitudes for the located earthquakes were calculated using the

total signal duration method: $M = a_0 + a_1 \log T$, where M is the magnitude, T, the total signal duration, and a_0 and a_1 are constants. Because no calibration data were available, the constants $a_0 = -1.01$ and $a_1 = 1.89$ arrived at by Real and Teng (1973) for microearthquakes in southern California were used. For the located earthquakes the signal durations for all stations were averaged. The calculated magnitudes ranged from -0.5 to 2.8.

b-values were determined by the maximum likelihood estimate method (Aki, 1965) for both the located events and for a detailed sample of local earthquakes at Cove Fort (Figure 14). The b-value obtained for the located earthquakes was $0.84 \pm .16$ (Figure 14a). Figure 14b indicates the magnitude-frequency relation for the localized earthquakes at the Dog Valley station. These events were generally very small, but a b-value of $1.27 \pm .18$ was obtained. A smaller value of 1.06 was arrived at by Smith and Sbar (1974) for the Intermountain Seismic Belt. If the degree of error for the b-values obtained from this survey is considered, values close to 1.06 could be rationalized.

Sykes (1970) has suggested that high b-values such as 1.3 on the mid-Atlantic ridge are in general indicative of swarm activity. The high b-value of 1.27 for earthquakes north of Cove Fort does not necessarily require swarm-like activity, but it does lend support to that proposition.

Earthquake swarms can be generated by concentrated stresses and inhomogeneities in the source rock (Mogi, 1967). Sykes (1970) has shown that high temperatures and high pore pressure in a small volume

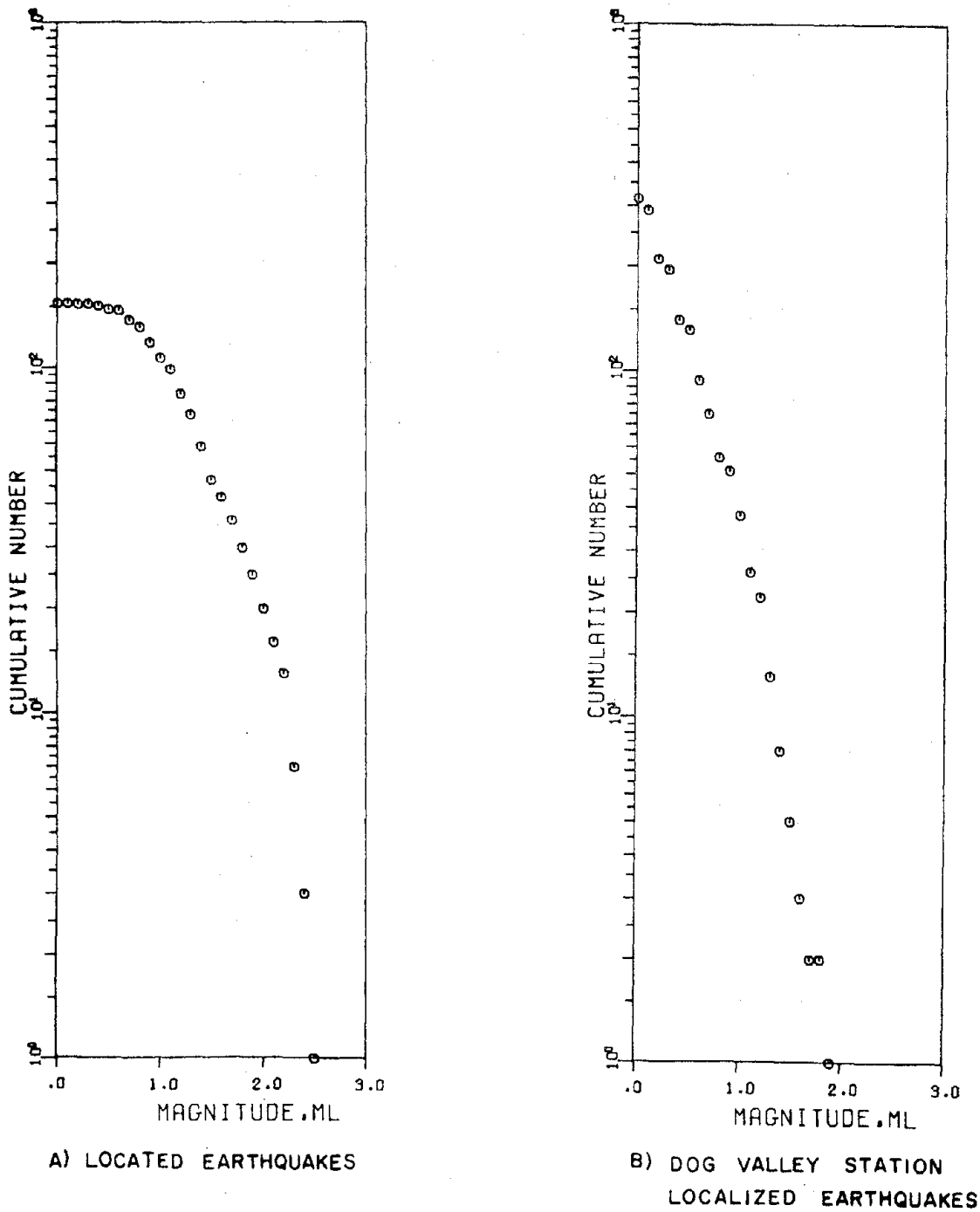

Figure 14
Frequency of occurrence plots.

of rock can produce concentrated stresses which in turn produce swarms. If the high b-values at Cove Fort indicate swarm activity, the high temperatures and pore pressures associated with the swarms most probably produce the hot water wells in Dog Valley and the sulphur springs at Sulphurdale (Crosby, 1959).

Fault Plane Solutions

Using lower-hemisphere, equal-area, stereographic projections, two composite fault plane solutions were determined for the earthquake activity near Cove Fort. No solutions could be made for other areas of the survey because of the lack of sufficient activity or inconsistency of focal mechanisms. Inconsistent solutions were obtained until only the most accurately located events with resolved focal depths and epicenters within a 5 km^2 area were used. Two separate solutions were determined using earthquakes 13 km southwest of Kanosh and 4 km northeast of Cove Fort (Figure 15).

Figure 16 shows the two composite fault plane solutions for the Cove Fort area. Fault plane solution 1 was compiled from eight earthquakes (Appendix C) 13 km southwest of Kanosh (Figure 16). The solution indicates normal faulting with a strike of N 22^{o} W and dipping 64^{o} NE (nodal plane 1), or N 48^{o} E and dipping 54^{o} NW (nodal plane 2). Crosby (1959) indicates northeast-trending normal faulting coincident with earthquakes used for this fault plane solution, suggesting nodal plane 2 to be the correct fault plane. Cross section B-B' shows no specific dipping zone to correlate with this fault plane solution.

Fault plane solution 2 (Figure 16) was compiled from eight earth-

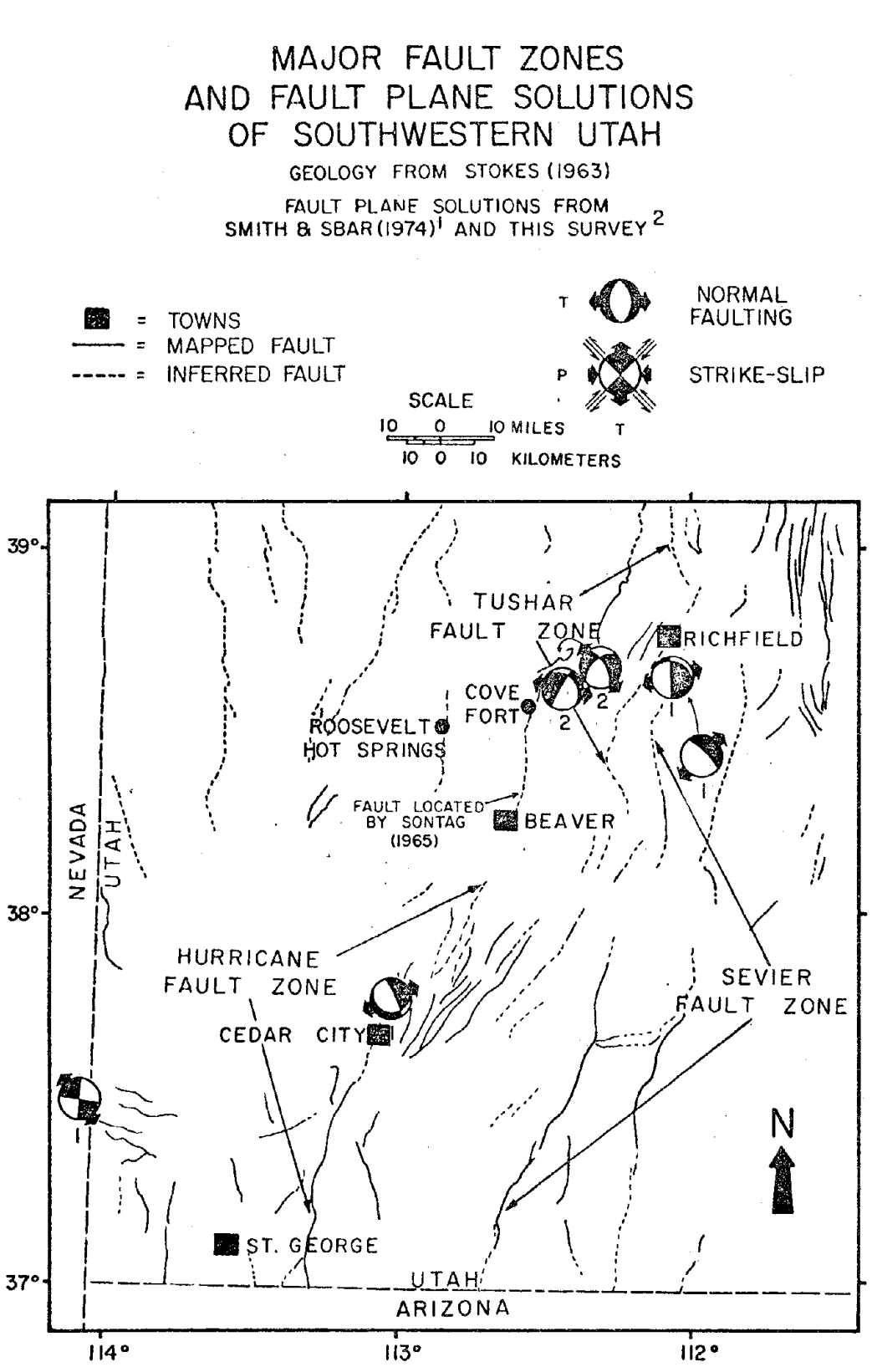

Figure 15
Fault plane solutions and fault zones of southwestern Utah.

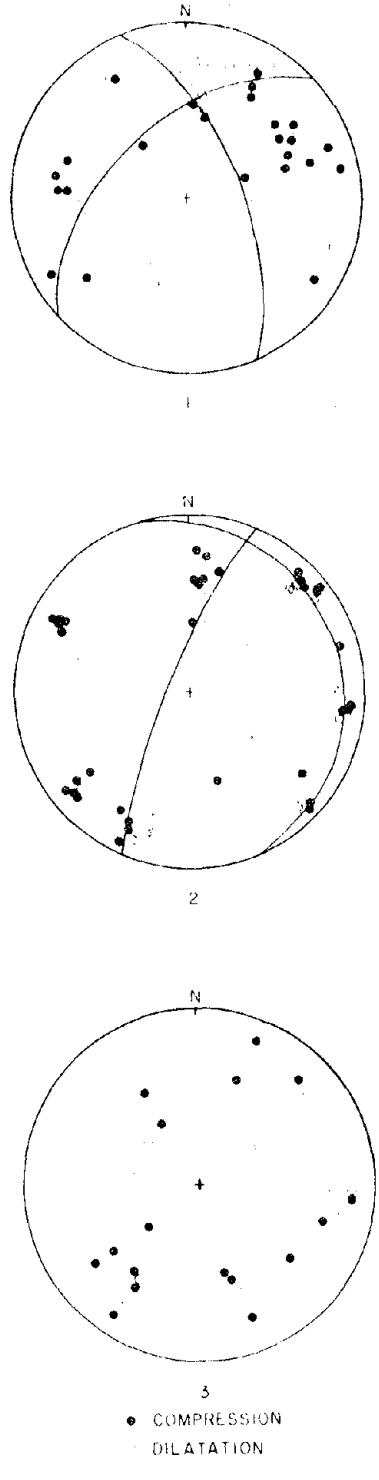

Figure 16
Composite fault plane solutions.

quakes 4 km northeast of Cove Fort (Appendix C). The composite fault plane solution has a steeply dipping fault plane of 80^{o} NW, striking N23^{o} E for nodal plane 1. Nodal plane 2 indicates a moderate dip of 14^{o} E striking N 20^{o} W. Cross section A-A' passes through this area, and suggests hypocenters along a zone dipping at 70^{o} W, thus implying nodal plane 1 as the correct fault plane.

A fault plane solution was attempted for the earthquakes west of Cove Fort. Only well-located earthquakes with clear first motions were used. These events (Appendix C) show no consistent focal mechanism either when they were plotted together, or when groups of earthquakes in close proximity were plotted separately (Figure 16).

Unresolved focal mechanisms have been encountered elsewhere. Caldwell and Frohlich (1975) obtained an inconsistent focal mechanism for the Alpine fault zone in New Zealand. The Alpine fault zone forms part of the boundary between the Indian and Pacific plates, and evidence of both right lateral motion and vertical movement are present (Caldwell and Frohlich, 1975). The area west of the Cove Fort is not along a major plate boundary, however, evidence of both strike-slip and vertical motion are present (Crosby, 1973, E. Clark, personal communication, 1976). The unresolved focal mechanism is most probably due to complex faulting of the area. If the earthquakes considered for the composite fault plane solution were associated with two or more faults of different orientation, such a complex would show no consistent first-motion patterns.

The T-axes of both solutions are generally oriented in an east-west direction (Table 1). Smith and Sbar (1974) have proposed that

Table 1. Data for composite fault plane solutions 1 and 2

COMPOSITE FAULT PLANE SOLUTION	1	2
LOCATION	Southwest of Kanosh	Cove Fort
TYPE OF FAULTING	Normal	Normal
NODAL PLANE 1 STRIKE/DIP	N 22^{o} W/64^{o} NE	N 23^{o} E/80^{o} NW
NODAL PLANE 2 STRIKE/DIP	N 48^{o} E/54^{o} NW	N 20^{o} W/14^{o} NE
P-AXIS AZIMUTH/PLUNGE	197^{o} SW/46^{o} SW	126^{o} SE/54^{o} SE
T-AXIS AZIMUTH/PLUNGE	110^{o} SE/14^{o} SE	285^{o} NW/34^{o} NW

the Great Basin subplate is moving westward with respect to the stable portion of the North American plate. The composite fault plane solutions of the Cove Fort area tend to support this westward movement. Fault plane solutions from Smith and Sbar (1974) for areas east of the surveyed area (Figure 15) also indicate general east-west T-axes orientations.

The fault plane solution from the southern Utah-Nevada border indicate strike-slip faulting to be present (Figure 15) with T-axes orientation southeast-northwest. Slemmons (1967) has shown that the faulting coincident with an east-west seismic zone from southwestern Utah, westward into Nevada, gradually increases in left-lateral components, which is in agreement with the fault plane solutions from Smith and Sbar (1974). Because of the east-west T-axes orientations, the fault plane solutions from this survey are probably assocaited with the Intermountain Seismic Belt, rather than the east-west zone of activity extending into southern Nevada. Perhaps if focal mechanisms could be resolved west of Cove Fort and west of the north edge of the Mineral Range, a different T-axes orientation would be found.

P-Wave Delays

P-wave velocities have been found to vary with rock type and densities (Richter, 1958). However, variations of P-wave velocities with high temperature zones are not conclusive since densities change with temperature as well. If a high temperature zone causes a decrease in P-wave velocity, we can investigate anomalous heat zones

by examining P-wave travel time residuals.

Figure 17a indicates an average positive P-residual for the Ranch Canyon station (RAN) of +0.1 sec. for an azimuth of 40^{o} to 60^{o}. The events showing a positive delay for RAN originated northeast of Cove Fort, and also show an equally strong positive residual at the Twin Peaks II station (TW2, Figure 17b). The azimuths for TW2 indicate a positive residual of +0.1 sec. from 110^{o} to 160^{o}. The North Mineral station (NOM) showed slightly positive residuals from the Cove Fort events (Figure 18a), however, the positive residuals for this station are not nearly so prominent as for RAN and TW2. The Sulphur Creek station (SLF) had a predominance of negative residuals from earthquakes northeast of Cove Fort (Figure 18b). These negative residuals are probably a function of the location of the epicenters, since three stations on the perimeter of the array had definite positive residuals.

The geometry of the positive delays of the stations is indicated in figure 19. The Mine (MIN), Cinder Crater (CIN), Antelope Valley (ANT) and Sandstone (SND) stations lie in the region between Cove Fort and the perimeter stations RAN, NOM, and TW2 (Figure 19). Because no delays above the RMS were observed at these intermediate stations, the anomalous low velocity zone is thought to be located between longitude 112^{o} 40' W and the outer stations RAN, NOM, and TW2. The anomalous zone must therefore include parts of the Mineral Range, and areas northeast of the Mineral Range.

The interpretation of P-wave residuals relies strongly upon the accuracy of the velocity model. If the true earth structure has dipping layers, the plane layer, non-dipping velocity model which we

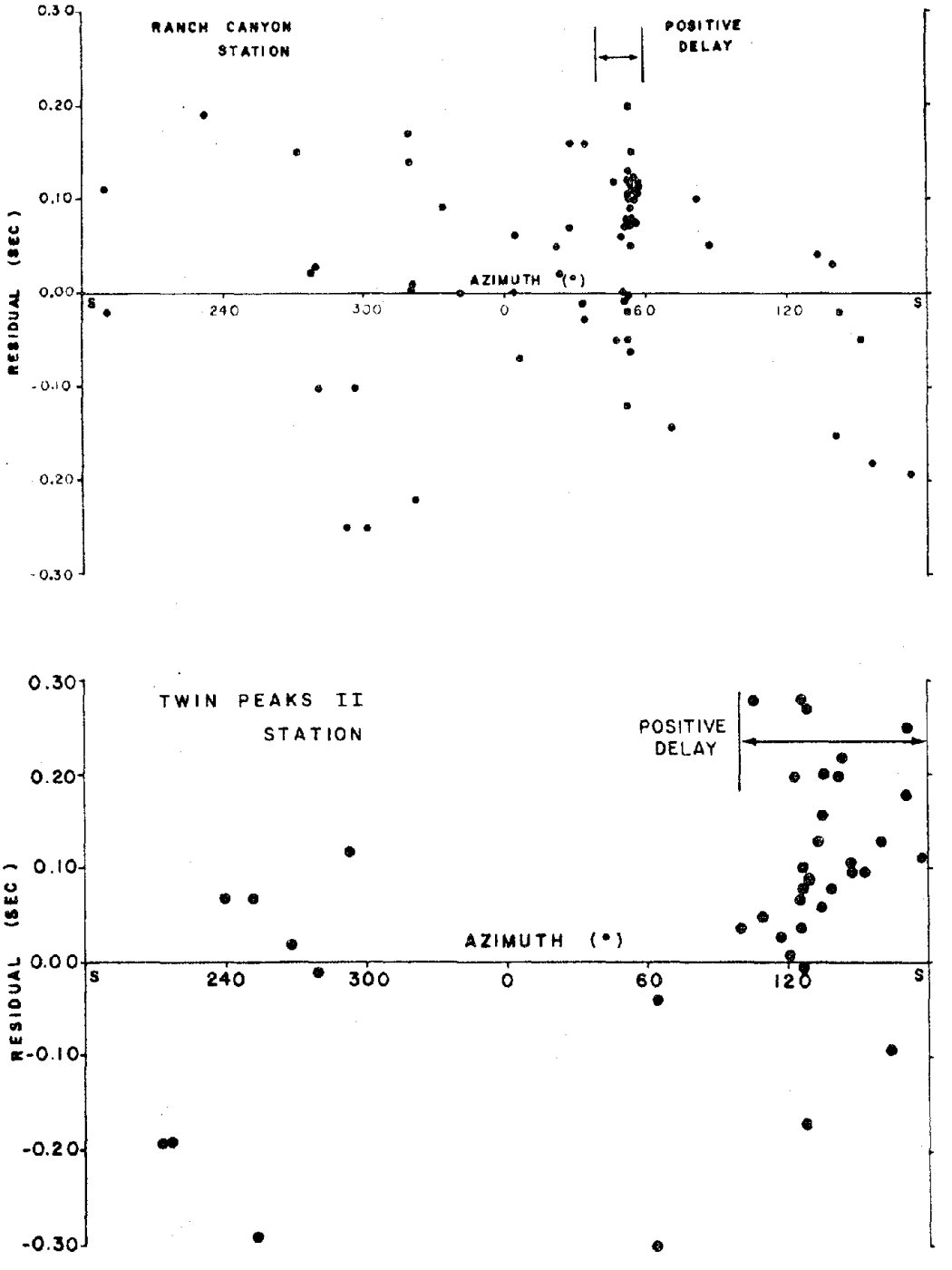

Figure 17
P-wave residuals for the Ranch Canyon and
Twin Peaks II Stations.

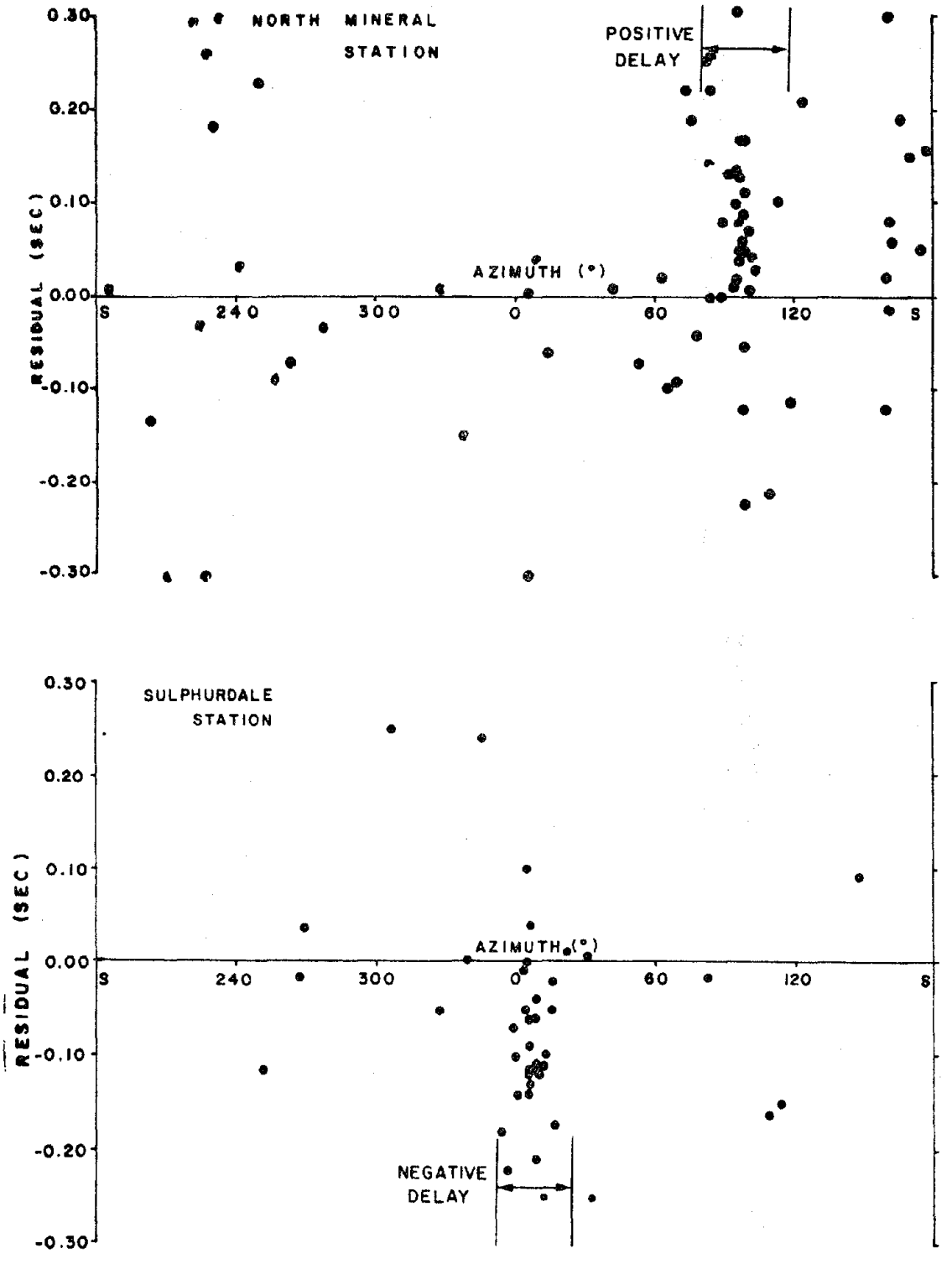

Figure 18
P-wave residuals for the North Mineral and Sulphur Creek Stations

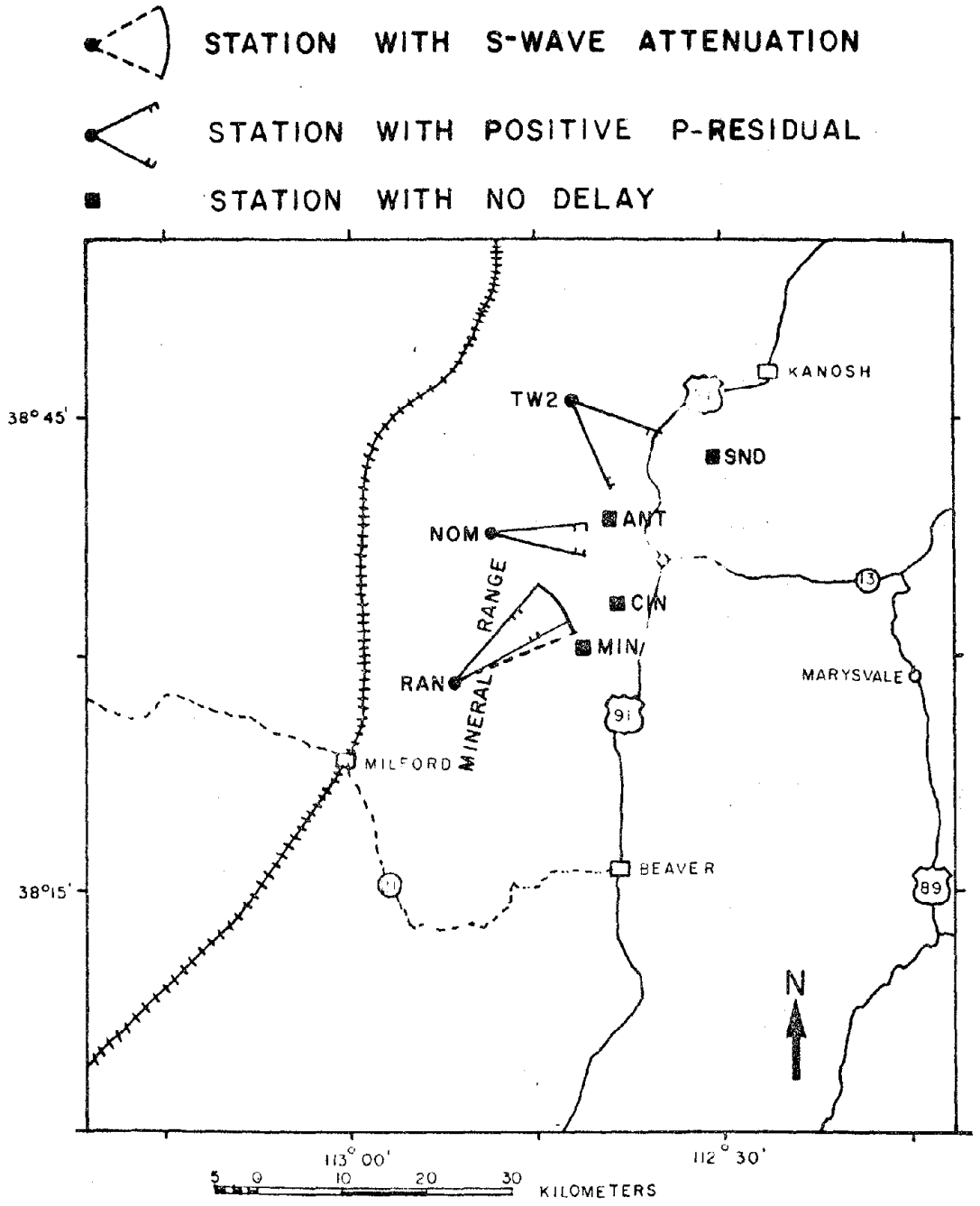

Figure 19
P-wave delay map.

have used could produce systematic residuals as a function of azimuth. The rays used in the residual analyses were primarily propagated in the second layer. Since the alluvial layer is only 1/2 km thick, a dip on this layer would be negligible in producing systemic residuals. A dip of the deeper layers, however, would have a pronounced effect. Also, layer thinning could cause systematic residuals, so we must interpret the residuals of the anomalous zone with caution.

Matumoto (1971) has used residuals and P and S-wave attenuation from microearthquakes to deduce the location of magma chambers at Mount Katmai National Monument, Alaska. Seismograms from the Roosevelt-Cove Fort area were examined for S-wave attenuation. Weak S-arrivals were found most consistently at the RAN station. Typical examples of prominent and weak S-phases for the RAN station are indicated in figure 20. In figure 21 epicentral distance of weak or no S-phase events and prominent S-phase events are plotted as functions of azimuth. Between azimuths 40^{o} to 65^{o}, 24 weak S-arrivals were found as opposed to 10 prominent S-phases for the same azimuth. Approximately 70 percent of the events having this azimuth were found to lack well developed S-phases. This coincides with the positive residuals within 5^{o} for RAN (Figure 17). Crebs (1976) and W. P. Nash (personal communication, 1976) have postulated that the volcanic domes of the Mineral Range overlie a magma chamber or a zone of partial melt. If this is the case, the observed S-wave attenuation may be associated with this zone.

The combined observations of positive P-wave residuals and S-wave

TYPICAL S-PHASE ARRIVALS AT THE RANCH CANYON STATION

PROMINENT S-PHASE

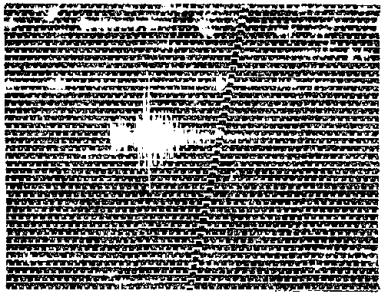

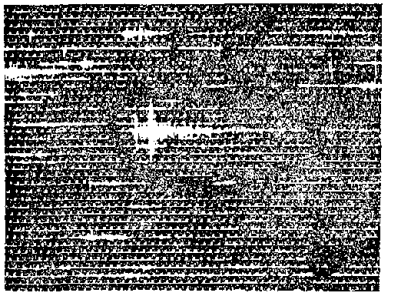

WEAK S-PHASE

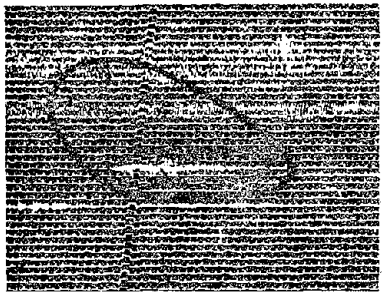

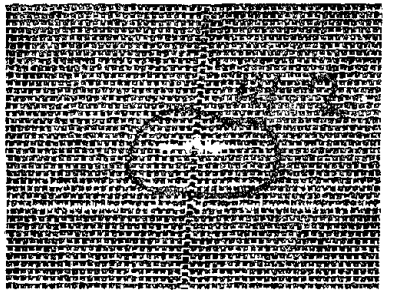

Figure 20
Sample S-phase arrivals at the Ranch Canyon Station.

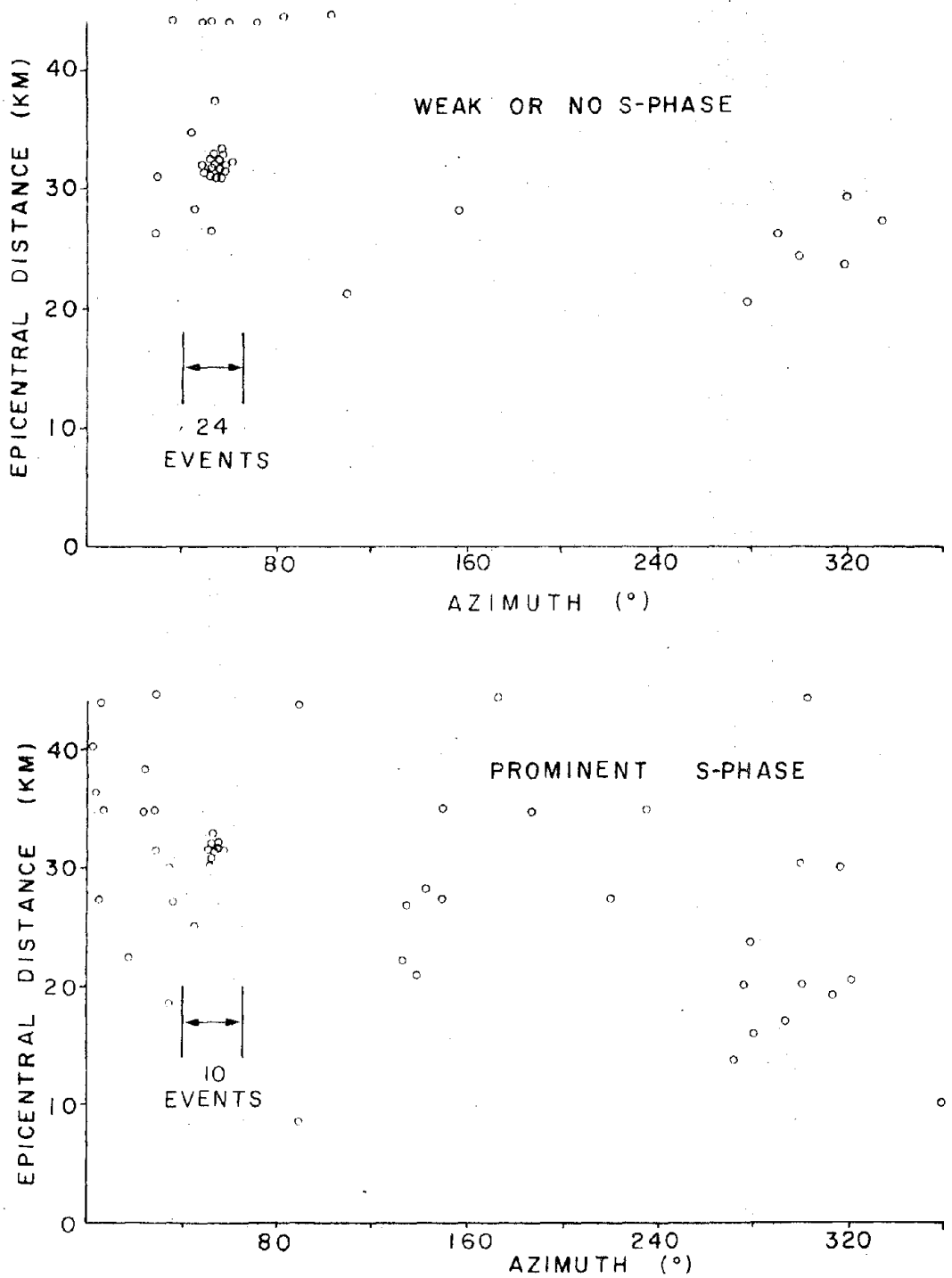

Figure 21
Weak and prominent S-phases at the Ranch Canyon Station.

attenuation seem to support the presence of a high-temperature zone in the central Mineral Range. If this zone exists, it is most likely the source of heat for the Roosevelt Hot Springs area.

STOCHASTIC MODELING

Probabilities relating numbers of shocks in a particular time period have long been of interest to seismologists (Richter, 1958). The major problem in applying statistical models is to account for all the variables which influence the system. Variables such as the cumulative energy of the system, creep, stick-slip, tidal strain, multiple events and a variable addition of potential energy can severely alter a model that may apply very well for one region, but not another.

Two points of view on the subject of the statistical process for the occurrence of earthquakes have received support. The first of these assumes that shocks of the same magnitude are Poisson independent and that λ, which is the rate of a specific magnitude occurrence, is only a function of magnitude. The probability of n shocks between magnitude M_o and $M_o + \Delta M$ occurring in a time interval t in length is:

$$P\left[N(t) = n,\ M_o<M<M_o + \Delta M\right]=\left[\frac{\lambda t\Delta M}{n!}\right]^n e^{-\lambda t\Delta M}$$

This model assumes that a normal earthquake occurrence is stationary and random with respect to time and that a number of shocks which occurs in a unit time is distributed in accordance with Poisson's law (Shimazaki, 1973, Knopoff, 1972). The probability of having a shock of magnitude between M and M + dM in an interval of time dt is $\lambda(M)dtdM$ (Shimazaki, 1973). In this way we remove the interrelation of shocks

of different magnitude in the same time interval. $\lambda(M)$ is given by the Gutenberg frequency-magnitude formula (Richter, 1958):

$$\log\lambda = a - bM$$

where a = 8.56 and b = 1.0. Several studies since the proposal of this model using Poisson's law have shown it not to be highly reliable (Knopoff, 1964, Udias and Rice, 1975).

Knopoff Model

The second and more popular point of view was suggested by Knopoff, (1971), and assumes that there is a state variable which is the potential energy of deformation of the seismic region. A successful application of this model to a volcanic earthquake swarm has been made by Filson and Simkin (1975). This method has been applied to the Cove Fort data.

The following brief description of this stochastic model is from Knopoff (1971). If we assume that deformational energy is a statistical variable, rather than having a sequence of discrete numerical quantities we will have a continuous function defined for all times t. So we let P(E,t)dE, be the probability that the energy of the region is between E and E + dE at time t.

All of the shocks will be considered to be instantaneous, even though in a real system they are of short duration compared to the time between events. Let α be the constant rate of addition of energy to the system; the potential energy is assumed to be derived from tectonic deformation along a fault or fault complex. $\lambda(E)dt$ will represent the probability that an earthquake will occur in an energy state

E between times t and t + dt. $T(X|E)dE$ is the conditional probability that if we are in the energy state X and if an earthquake occurs the region drops to an energy state between E and E + dE. E_{max} will represent the maximum energy the system can withstand.

To find $P(E,t)dE$ we must find the sum of two terms, i.e. there are two possible ways to arrive at an energy state E. The first is the probability that the system is in the energy state $E - \alpha dt$ at time $t - dt$ and passes into energy state E by the elapse of time dt without an earthquake. The second way is to assume the system is in a higher energy state X and then by the occurrence of an earthquake it drops into energy state E. The probability of this situation occurring in a given energy state X is $P(X,t)\lambda(X)T(X|E)(dt)(dE)(dX)$, Knopoff, (1971), but of course we must sum all possible states X between E and E_{max} thus:

$$P(E,t)dE = \{1 - \lambda(E)dt\}P(E - \alpha dt,\ t - dt)dE + \int_E^{E_{max}} P(X,t)\lambda(X)T(X|E)\,dXdtdE \qquad \text{eq. (1)}$$

The first term in the right hand member of equation (1) can be expanded in a Taylor series in the arguments t and E, and neglecting terms of higher order than 1 yields:

$$\lambda(E)P(E,t) + \alpha\frac{\partial P(E,t)}{\partial E} + \frac{\partial P(E,t)}{\partial t} = \int_E^{E_{max}} P(X,t)\lambda(X)T(X|E)dX, \qquad \text{eq. (2)}$$

which is the Kolmogorov Backward Equation (Kolmogorov, 1931).

If we only pursue the study of stationary processes, then $P(E,t)$ is independent of t (Baht, 1969), and equation (2) becomes:

$$\lambda(E)P(E) + \alpha \frac{dP(E)}{dE} = \int_{E}^{E_{max}} P(X)\lambda(X)T(X|E)dX. \qquad \text{eq. (3)}$$

The data that were used in the test of the model consisted of events detected at the Dog Valley station (Figure 10). Many of the earthquakes that were considered do not have located hypocenters because they did not appear on three or more stations. However, S minus P times (Figure 13) indicated that all of these events were within a radius of 15 km of the station and we assume had the same source mechanism. Magnitudes for all events were calculated as before, using the total signal duration method.

Seismic energy release was calculated for each event using the magnitude-seismic energy relation of Bath(1973):

$$\log_{10}E = 12.24 + (1.44)(M),$$

where M is the magnitude and E the energy release in ergs.

Filson and Simkin (1975), in applying the Knopoff model, examined a caldera block and made the assumptions that seismic efficiency is independent of magnitude, and seismic energy release reflects the rate at which potential energy was supplied. Although the Cove Fort area is definitly under a different tectonic regime, skeptically we are forced to make similar assumptions in order to apply the model.

The cumulative energy release for four week recording period is indicated in figure 22, and is plotted using a linear scale. It was desired to examine a period of time in which a relatively constant addition of energy was being released by a large number of events of near the same magnitude. This was done to find the linear constant α referred to above. Two large "jumps" in energy release are apparent

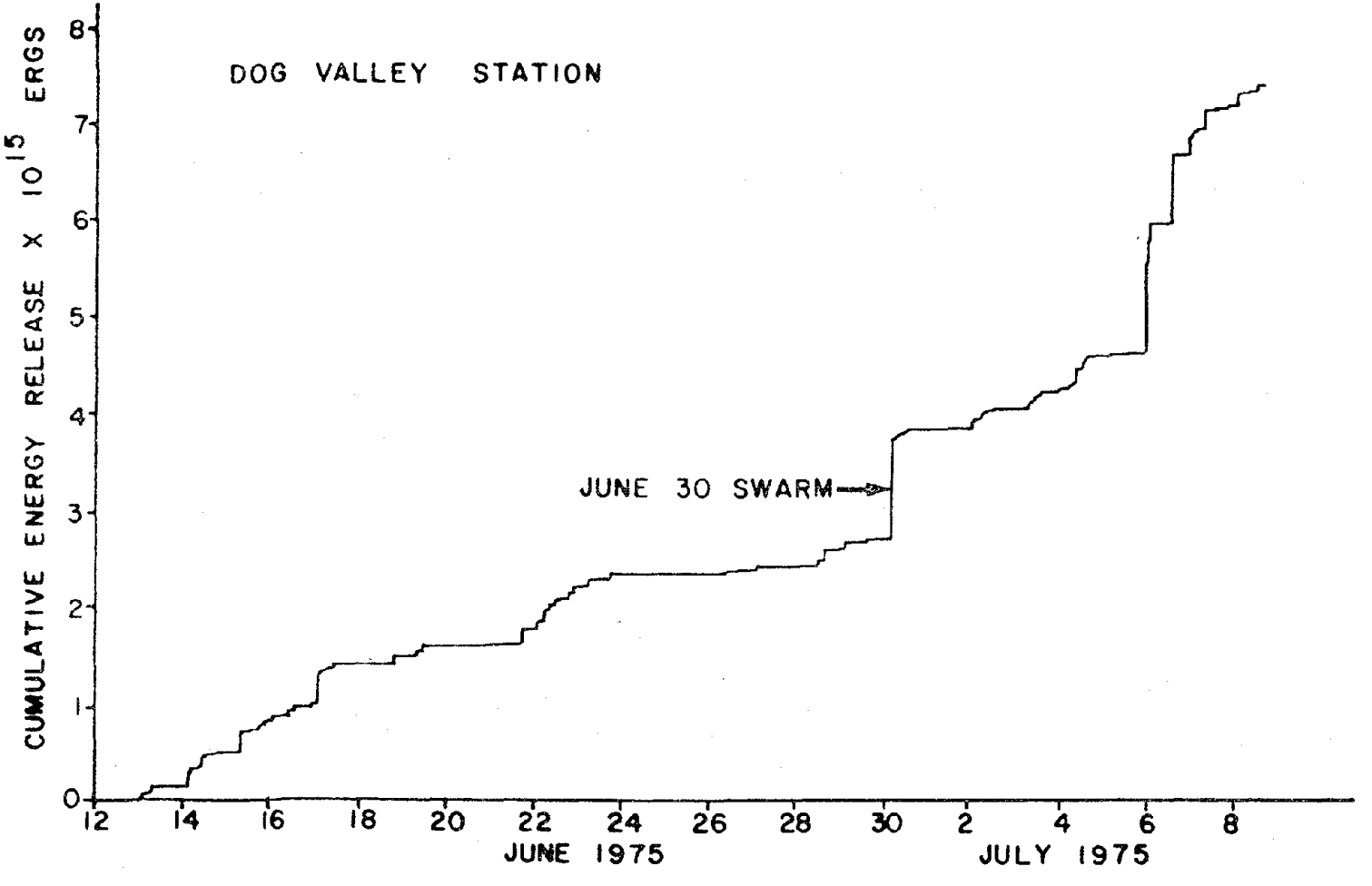

Figure 22
Cumulative energy release for the 1975 Cove Fort survey.

from figure 22, the first occurred on June 30, 1975 and the second was on July 6, 1975. The July 6 increase was due to three large events ranging up to M_L 2.1; however, the June 30 increase was due to a cluster of 51 events of almost equal magnitude.

The June 30 cluster was examined in greater detail and the cumulative energy release was plotted both linearly and logarithmically in figure 23. The period between 0400 to 0500, June 30 GMT was selected for analysis because the addition of energy was near constant.

E_{max} was taken to be the energy released from the largest earthquake of the cluster which was of magnitude 1.6. The minimum energy was taken to be zero, and the range of energy states from 0 to the cumulative energy at E_{max} were divided into 12 levels of 5.0×10^{13} ergs each.

The energy accumulation rate, α, was arrived at by making a linear least squares regression analysis of the linear cumulative energy plot (Figure 23a). The value obtained was $\alpha = 3.8 \times 10^{11}$ ergs/sec. or $\alpha = 5.7 \times 10^{12}$ ergs/15 sec.

The energy of the system at every 15 sec. interval was estimated using

$$E(t) = E_0 + \alpha t - \sum_{t=0}^{t-1} E_s, \qquad \text{eq.(6)}$$

after Filson and Simkin (1975), where E_0 is the initial energy at t=0, t is the number 15 sec.-time periods, and the summation indicates energy lost due to earthquakes previous to time t.

Each E(t) was then placed in one of the 12 energy levels and P(E) was calculated by counting the total number of entries in each energy

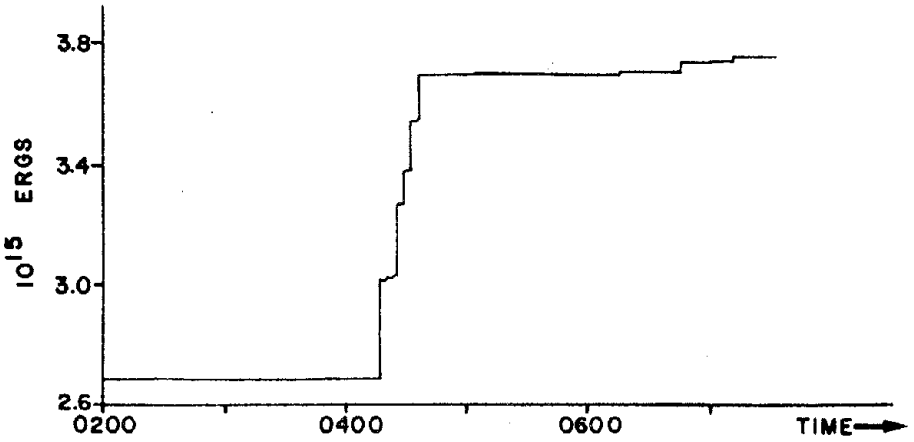

A) CUMULATIVE ENERGY RELEASE PLOTTED LINEARLY

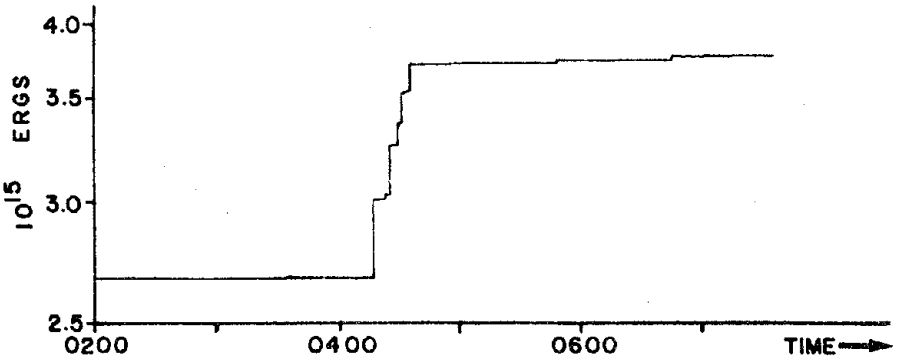

B) CUMULATIVE ENERGY RELEASE PLOTTED LOGARITHMICALLY

ENERGY RELEASE FOR THE JUNE 30, 1975 SWARM AT THE DOG VALLEY STATION

Figure 23

level. Figure 24a indicates a reasonably symmetric histogram for P(E).

$\lambda(E)$ was computed by examining the energy state for each 15 sec. interval, and whether or not an earthquake occurred. Figure 24b shows the probabilities computed for $\lambda(E)$.

Normalizing P(E) such that:

$$\int_0^{E_{max}} P(X)dX = 1,$$

(Hogg and Craig, 1970) the left-hand side of equation 3 was evaluated. The highest value obtained (figure 25) was for energy level 5, and the curve has some degree of symmetry. An entry for energy level 7 was not possible since $\lambda(E)$ takes on the value of 0 there.

The conditional probabilities T(X|E) were attempted in order to fully test the right hand side of equation 3. The following difficulties, however were encountered:

1. Since there were only 4 events which caused a change in energy levels, only 16 of the 144 conditional probabilities calculated had a value different from 0.

2. To compute the normalization of T(X|E) we must have the condition (Hogg and Craig, 1970):

$$\int_0^X T(X|E)dE = 1.$$

This caused the 16 conditional probabilities to increase to levels which made equation 3 not meaningful.

thus, the right hand side of equation 3 could not meaningfully be compared to the left hand side.

Fine energy level divisions were considered as a solution, but this produced an unnecessary bias on P(E) because of the small number of events considered. The ultimate solution to the problem would be to consider several clusters of events over a much longer time period.

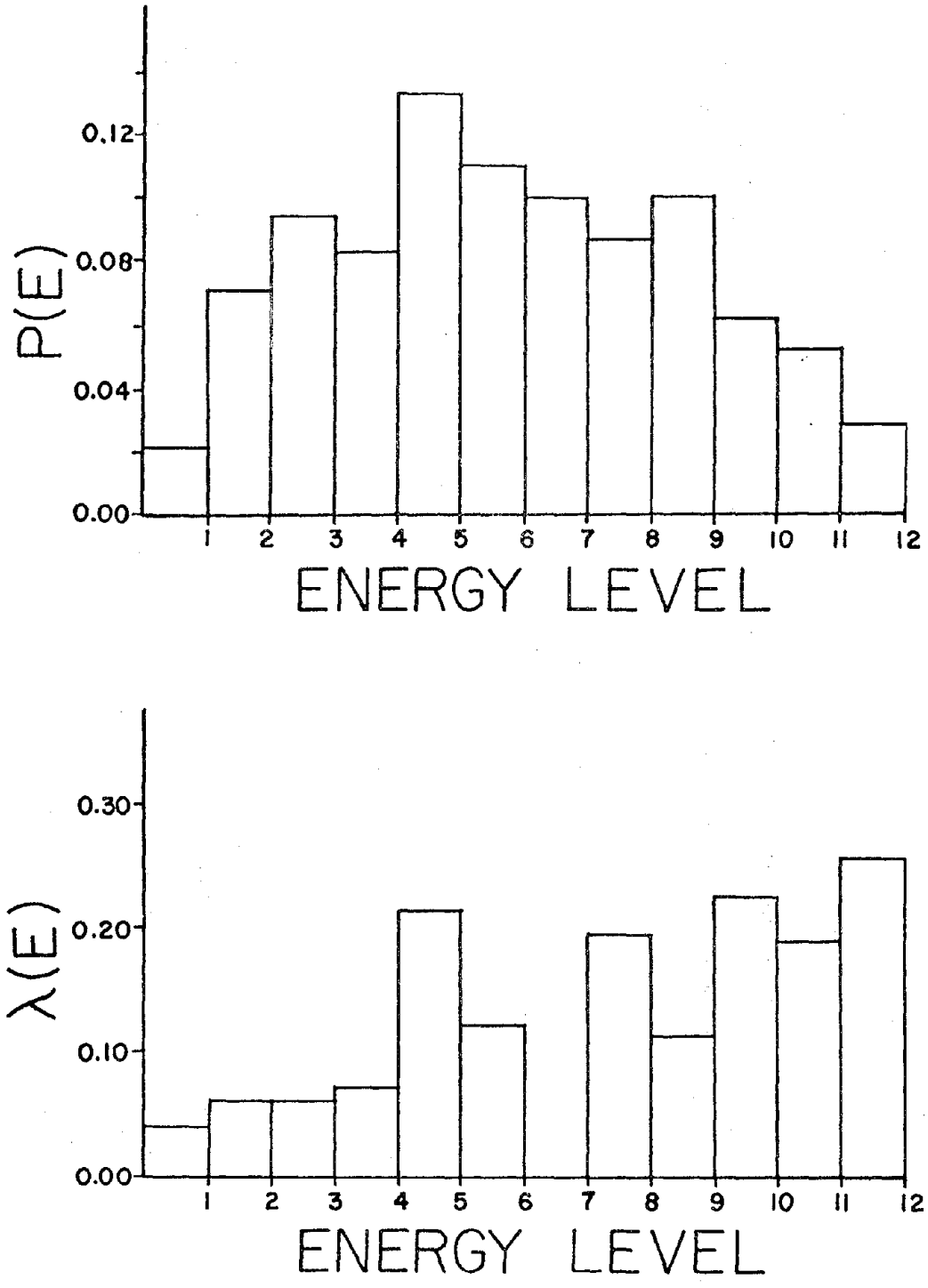

Figure 24
Probabilities of earthquake occurrence and energy states.

Histograms showing the distribution of P(E) (probability of being in a given energy level) and $\lambda(E)$ (probability of earthquake occurrence) against energy levels in multiples of 5.0×10^{13} ergs.

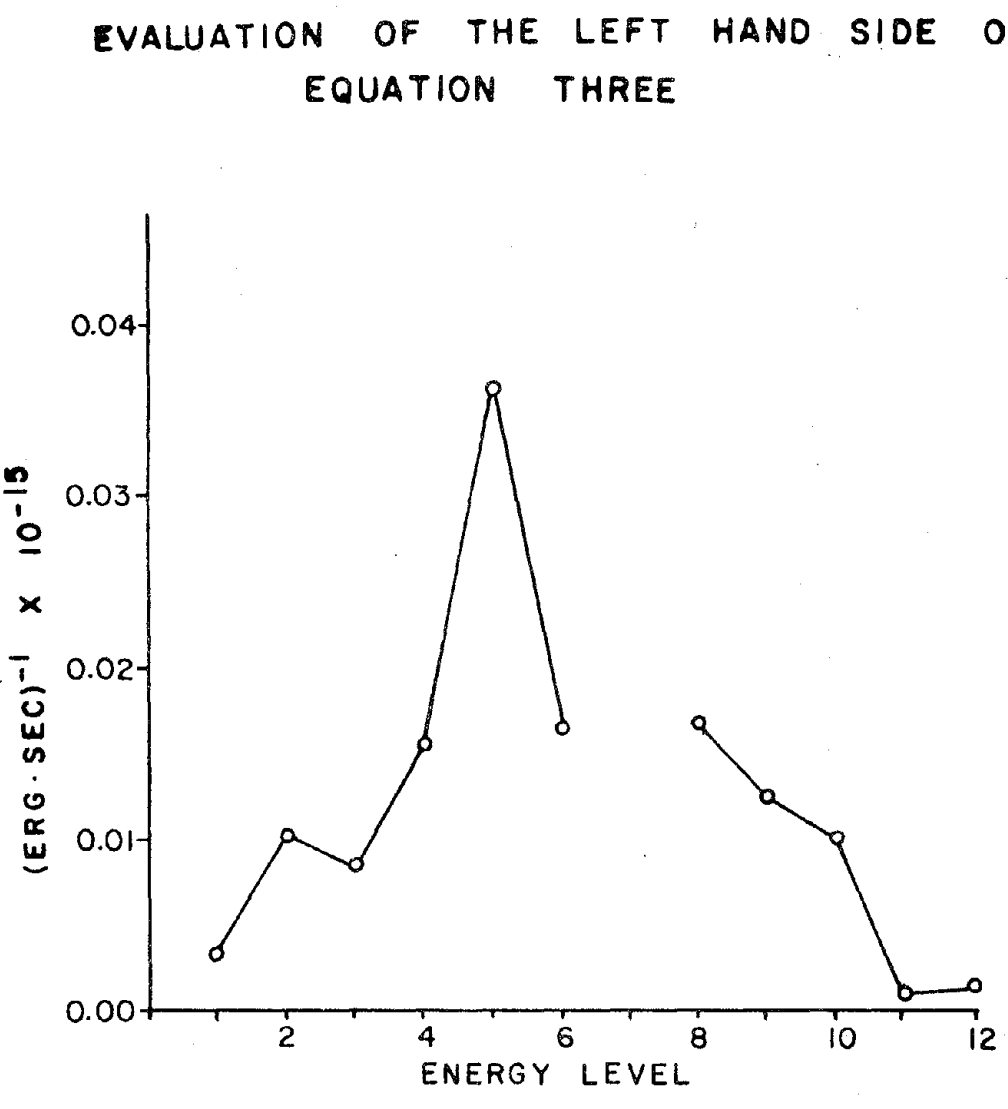

Figure 25
Evaluation of the Knopoff model.

However, many meaningful conclusions may be ascertained from the computations already made.

The nearly symmetric distribution of P(E) (Figure 24a) indicates that the system expended more time and was much more likely to be found in an intermediate energy state. The average magnitude of earthquakes occurring in energy levels 3 through 8 was 0.6. Larger or much smaller earthquakes seemed more prone to occur in one of the extreme energy levels 1 through 3 or 9 through 12.

The distribution of $\lambda(E)$ (Figure 24b), tends to increase with higher energy states. This indicates that the higher energy levels have a greater liklihood of earthquake occurrence. The noticeably low value in energy level 7 may be attributed to the short period of time under examination.

The approximate symmetry of P(E) and general increase in $\lambda(E)$ are consistent with swarm activity investiged by Filson and Simkin (1975). This analysis supports the proposition that this Cove Fort cluster of earthquakes is swarm-like in nature.

The case considered is for a small period of time only. The fit of the model is not excellent; however, the tectonic setting near Cove Fort is indeed complex (Clark, 1976). The inconsistencies encountered could easily be attributed to the complicated fault complexes, or the loss of deformational energy through some other means.

The application of the Knopoff model, along with high b-values supports the implication of swarm activity in the Cove Fort area. Mogi (1963) showed that swarm activity usually occurs at remarkably fractured regions, so high stress concentrations appear around numerous cracks and faults. Thus, local fractures begin to appear under low stress and

no singly large fracture can occur. Mogi (1963) further shows that swarms occur primarily in volcanic regions because of concentrated stress build-up in heterogeneous material and complex fracture zones. Since the Cove Fort area has a history of high volcanic activity, it is by no means improbable that the swarm activity is closely related to a volcanic source.

CONCLUSIONS

Earthquake surveys conducted around the Roosevelt Hot Springs KGRA and the Cove Fort - Sulphurdale KGRA, located a prominent zone of earthquake activity that extends north from Cove Fort to Kanosh. This trend of activity is coincident with the trend of the Intermountain Seismic Belt. Because of high b-values, and the relatively good fit of the Knopoff model, the activity at Cove Fort was characterized as swarm-like. Earthquake swarms have been shown to be closely related to volcanic activity, which could be interpreted to be responsible for the hot-water wells and hot springs in the area. Larger and smaller magnitude events were found to be more closely associated with either low- or high-energy states. The likelihood of earthquake occurrence was generally greater for high energy states. From historical seismicity and this survey, the earthquake hazard for the Cove Fort-Sulphurdale KGRA seems higher than for the Roosevelt area, and any future geothermal venture for the Cove Fort area must take this characteristic into account.

Fault plane solutions for the Cove Fort and Kanosh areas indicate primarily normal faulting with generally east-west trending T-axes. A focal mechanism for the area west of Cove Fort was not resolved. The explanation offered for the unresolved solution is the presence of a complex faulted upper-crust that does not relieve strain in a systematic manner.

The Roosevelt Hot Springs area was found to be anomalously low in

earthquake activity, however, during our two recording periods totaling 49 days, six events were located along the west flank of the Mineral Range. Four likely hypotheses, stable sliding, episodic seismic activity, an area of hot rock unable to support stress, and a quiescent seismic zone are proposed as an explanation for the lack of seismic activity at the Roosevelt Hot Springs KGRA.

Consistent positive P-residuals up to +0.13 sec. and detectable S-wave attenuation at the RAN station site closest to the Roosevelt Hot Springs area, suggest the presence of a low-velocity upper-crustal layer beneath the Mineral Range. This may be produced by high temperatures that would enhance stable sliding instead of stick-slip movement (Brace and Byerlee, 1970). Perhaps the Roosevelt Hot Springs area is characterized by short periods of episodic activity separated by periods of quiescence, and the recording period was too short to sample the true seismic state.

If the recording period was too short at Roosevelt, long-term seismic monitoring could provide a more definitive test of the temporal seismicity, and give important information on possible fault controlled permeability of the geothermal model. If a geothermal power plant is eventually established at the Roosevelt area, geothermal fluid injection or withdrawal could significantly vary the strain energy sufficiently to induce earthquakes. A permanent seismograph array could give warning of increased seismic activity.

REFERENCES

Aki, K., 1956, Some problems in statistical seismology: Zixin, vol. 8, p. 205-228 (Translation, A.S. Furumoto, 1963).

Baht, U.N., 1972, Elements of applied stochastic processes: John Wiley and Sons, Inc., New York, New York.

Bath, M., 1973, Introduction to Seismology: John Wiley and Sons, Inc., New York, New York.

Berge, C. W., Crosby, G. W., and Lenzer, R. C., 1975, Geothermal exploration of Roosevelt KGRA, Utah: New Concepts of Exploration in the Rockies, AAPG and SEPM 25th An. mtg., no. 66, p. 52-53.

Blackwell, D. D., and Bagg, C., 1973, Heat flow in a "blind" geothermal area near Marysville, Montana: Geophysics, vol. 38, no. 5, p. 941-956.

Brace, W. F. and Byerlee, J. D., 1970, California earthquakes: Why only shallow focus?: Science, vol. 168, p. 1573-1575.

Brune, J. N. and Allen, C. R., 1967, A microearthquake survey of the San Andreas fault system in southern California: Bull. Seismol. Soc. Am., vol. 57, p. 277-296.

Caldwell, J. G. and Frohlich, C., 1975, Microearthquake study of the Alpine fault zone near Haast, South Island, New Zealand: Bull. Seismol. Soc. Am., vol. 65, no. 5, p. 1097-1104.

Clark, E., 1976, Geology of north central Beaver County, Utah: unpub. M. S. thesis, Brigham Young University, in prep.

Condie, K. C., 1960, Petrogenesis of the Mineral Range pluton, southwestern Utah: unpub. M. A. thesis, University of Utah, 94 p.

Cook, K. L., Montgomery, J. R., Smith, J. T. and Gray, E. F., 1975, Simple Bouguer gravity anomaly map of Utah: Utah Geol. and Mineral Survey map 37.

_____, and Smith, R. B. 1967, Seismicity in Utah, 1850 through June 1965: Bull. Seis. Soc. Am., vol. 57, no. 4, p. 689-718.

Crebs, T. J., 1976, Regional gravity survey of the central Mineral mountains, Utah including detailed gravity and ground magnetic survey of the Roosevelt Hot Springs area: unpub. M. S. thesis, University of Utah, in prep.

Crosby, G. W., 1959, Geology of the southern Pavant Range, Millard and Sevier Counties, Utah: unpub. M. S. thesis, Brigham Young University, 59 p.

_____, 1973, Regional structure in southwestern Utah: Geology of the Milford area 1973, Utah Geological Association publication 3, p. 27-32.

Earll, F. N., 1957, Geology of the central Mineral Range, Beaver County, Utah: unpub. Ph.D. thesis, University of Utah, 112 p.

Eaton, G. P., 1975, Characteristics of a transverse crustal boundary in the Basin and Range province of southern Nevada in Abstracts with Programs: Geol. Soc. Am., vol. 7, no. 7, p. 1063-1064.

Filson, J. and Simkin, T., 1975, An application of a stochastic model to a volcanic earthquake swarm: Bull. Seismol. Soc. Am., vol. 65, no. 2- p. 351-357.

Friedline, R. A., Smith, R. B., and Blackwell, D. D., 1976, Seismicity and contemporary tectonics of the Helena, Montana area: Bull. Seismol. Soc. Am., vol. 66, no. 1, p. 81-95.

Gibowicz, S. J., 1973, Variation of the frequency-magnitude relation during earthquake sequences in New Zealand: Bull. Seismol. Soc. Am., vol. 63, no. 2, p. 517-528.

Godwin, L. H., Haigler, L. B., Rioux, R. L., White, D. E., Muffler, L. J. P., and Wayland, R. G., 1971, Classification of public lands valuable for geothermal steam and associated geothermal resources: U. S. Geol. Survey Circ. 647, 18 p.

Hamilton, R. M., and Muffler, L. J. P., 1972. Microearthquakes at the Geysers geothermal area, California: J. Geophys. Res., vol. 72, no. 11, p. 2081-2086.

Heylmun, E. B., 1966, Geothermal power potential in Utah: Utah Geol. and Mineral Survey spec. studies 14, 28 p.

Hintze, L. F., ed., 1963, Geologic map of southwestern Utah: Utah State Land Board, scale 1:250,000.

Hogg, R. V., and Craig, A. T., 1970, Introduction to mathematical statistics, 3rd edition: Macmillan Publishing Co., Inc., New York, New York.

Knopoff, L., 1964, The statistics of earthquakes in southern California: Bull. Seismol. Soc. Am., vol. 54, no. 6, p. 1871-1873.

_____,1971, A stochastic model for the occurrence of main-sequence earthquakes: Rev. Geophys. Space Phys., vol. 9, no. 1, p. 175-188.

_____, Mitchel, R., and Jackson, D., 1972, A stochastic analysis of a model earthquake sequence: Geophys. J., vol. 29, p. 255-261.

Kolomogorov, A., 1931, Über die analytischen Methoden in der Wahrscheinlichkeitrechnung: Math. Ann., vol. 104, p. 415-458.

Lange, A. L., and Westphal, W. H., 1969, Microearthquakes near the Geysers, Sonoma County, California: J. Geophys. Res., vol. 74, p. 4377-4378.

Lee, W. H. K., and Lahr, J. C., (1972), HYPO71 a computer program determining hypocenter, magnitude and first motion pattern of local earthquakes: U. S. Geological Survey open file report, 100 p.

Lee, W. T., 1906, The Cove Creek sulphur beds, Utah: U.S. Geological Survey Bull. 315, p. 485-489.

Liese, H. C., 1957, Geology of the northern Mineral Range, Millard and Beaver counties: unpub. M. S. thesis, University of Utah, 88 p.

Matumoto, T., 1971, Seismic body waves observed in the vicinity of Mount Katmai, Alaska, and evidence of molten chambers: Geol. Soc. Am. Bull., vol. 82, p. 2905-2920.

McNitt, J. R., 1965, Review of geothermal resources; in Lee, W. H. K. ed., Terrestrial heat flow: Am. Geophy. Union Geophys., Mon. Ser. No. 8, p. 240-266.

Mehnert, H., 1975, In personal communication to Dr. W. P. Nash from P. D. Rowley, U. S. Geological Survey, November, 1975.

Michaels, P., 1973, An application of the generalized linear inverse method to the location of microearthquakes and simultaneous velocity model determination: unpub. M. S. thesis, University of Utah, 187 p.

Mogi, K., 1963, Some discussions on aftershocks, foreshocks, and earthquake swarms: Bull. Earthquake Res. Inst., vol. 41, p. 615-658.

_____, 1967, Earthquakes and fractures: Tectonophysics, vol. 5, p. 35-55.

Mueller, S., and Landisman, M., 1971, An example of the unified method of interpretation for crustal seismic data: Geophys. J. Roy. Astron. Soc., vol. 23, p. 365-371.

Peterson, C. A., 1975, Geology of the Roosevelt Hot Springs area, Beaver County, Utah: Utah Geology, vol. 2, no. 2, p. 104-116.

Pitt, A. M., and Steeples, D. W., 1975, Microearthquakes in the Mono Lake-Northern Owens Valley, California, region from September 28, to October 18, 1970: Bull. Seismol. Soc., Am., vol. 65, no. 4, p. 835-844.

Real, C. R., and Teng, T-L., 1973, Richter magnitude and total signal duration: Bull. Seismol. Soc. Am., vol. 63, no. 5, p. 1809-1827.

Richter, C. F., 1958, Elementary Seismology: W. H. Freeman and Co., San Francisco.

Sbar, M. L., Baranzangi, M., Dorman, J., Scholz, C., and Smith, R. B., 1972, Tectonics of the intermountain seismic belt, western United States; microearthquakes seismicity and composite fault plane solutions: Geol. Soc. Bull., vol. 83, p. 12-28.

Shimazaki, K., 1973, Statistical method of detecting unusual seismic acitivities: Bull. Seismol. Soc. Am. vol. 63, no. 3, p. 969-982.

Shuey, R. T., 1974, Aeromagnetic map of Utah: Department of Geology and Geophysics, University of Utah, and Utah Geological and Mineral Survey.

Slemmons, D. B., 1967, Pliocene and Quaternary crustal movements of the Basin and Range Province, USA: J. Geosciences, Osaka City University, vol. 10, Art 1-11, p.91-103.

Smith, R. B., and Sbar, M. L., 1974, Contemporary tectonics and seismicity of the western United States with emphasis on the intermountain seismic belt: Geol. Soc. Am., vol. 85, p. 1205-1218.

_____, 1975, Seismicity, crustal structure, and Cenozoic tectonics of the Basin and Range, Rocky Mountains, and Colorado Plateau in Abstracts with Programs: Geol. Soc. Am., vol. 7, no. 7, p. 1277.

Sontag, R. J., 1965, Regional gravity survey of parts of Beaver, Millard, Piute and Sevier Counties, Utah: unpub. M. S. thesis, University of Utah, 30 p.

Steeples, D. W., and Pitt, A. M., 1976, Microearthquakes in and near Long Valley, California: J. Geophys. Res., vol. 81, no. 5, p. 841-847.

Stokes, W. L. ed., 1963, Geologic map of Utah: Utah State Land Board, scale 1:250,000.

Sykes, L. R., 1970, Earthquake swarms and seafloor spreading: J. Geophys. Res., vol. 75, p. 6598-6611.

Thangsuphanich, I., 1976, Regional gravity survey over the southern Mineral Range: unpub. M. S. thesis, University of Utah, 37 p.

Trimble, A. B., and Smith, R. B., 1975, Seismicity and contemporary tectonics of the Yellowstone Park-Hebgen Lake region: J. Geophys. Res., vol. 80, p. 733-741.

Udias, A., and Rice, J., 1975, Statistical analysis of microearthquake activity near San Andreas Geophysical Observatory, Hollister, California: Bull. Seismol. Soc. Am. vol. 65, no. 4, p. 809-827.

United States Department of Commerce, 1974, Federal Register: vol. 36, p. 6441.

United States Department of Commerce, 1975, Federal Register: vol. 39, p. 28545, vol. 40, p. 3234, 19026.

Ward, P. L., 1972, Microearthquakes: Prospecting tool and possible hazard in the development of Geothermal Resources: Geothermics, vol. 1, p. 3-12.

_____, and Bjornson, S., 1971, Microearthquakes swarms and the geothermal areas of Iceland: J. Geophys. Res., vol. 76, p. 39-53-3982.

Williams, J. S., and Tapper, M. L., 1953, Earthquake history of Utah, 1850-1949: Bull. Seismol. Soc. Am., vol. 43, no. 3, p. 191-218.

Willard, M. E., and Callaghan, E., 1962, Geology of the Marysvale quadrangle, Utah: U. S. Geol. Survey Geol. Quad. map GQ-154.

Wyss, M., 1973, Toward a physical understanding of the earthquake-frequency distribution: Geophys. J. R. Act. Soc., vol. 31, p. 340-359.

Zimmerman, J. T., 1961, Geology of the Cove Creek area; Millard County and Beaver County, Utah: unpub. M. S. thesis, University of Utah, 91 p.

APPENDIX A

Listing of Located Earthquakes

Units Used in Appendix A

Time: hours, minutes, seconds
in Greenwich Mean Time

Depth: km

RMS: sec

EVENT NO	DATE	TIME	LATITUDE	LONGITUDE	DEPTH	MAG	RMS
1	740907	1432 19.69	38 34.06	112 43.55	5.006	1.55	.06
2	740907	2055 39.26	38 35.42	113 1.55	5.006	1.81	.79
3	740909	1718 22.61	38 43.75	112 22.68	10.00	1.10	.93
4	740909	2132 32.96	38 30.57	112 52.41	5.006	1.84	.00
5	740911	1605 11.58	38 34.08	112 49.81	5.006	1.12	.27
6	740912	2053 36.10	38 33.99	112 51.96	5.006	.98	.21
7	740912	2128 59.74	38 20.59	112 43.18	.88	1.63	.12
8	740913	148 22.25	38 29.85	112 20.56	10.00	.55	1.03
9	740913	808 16.78	38 31.04	112 41.37	5.006	1.46	.26
10	740913	1541 39.98	38 38.16	112 50.71	1.16	1.75	.37
11	740913	1819 33.69	38 26.85	113 4.55	.67	1.34	.09
12	740913	1854 27.64	38 37.20	112 46.39	5.006	.94	.47
13	740913	1915 47.86	38 11.78	112 43.13	5.006	1.60	.07
14	740913	2020 27.98	38 39.15	112 39.30	5.006	1.60	.07
15	740913	2049 8.45	38 23.60	112 46.40	5.006	1.27	.30
16	740913	2158 55.40	38 37.02	113 3.03	1.80	1.24	.07
17	740913	2159 20.09	38 25.88	113 .44	5.006	1.29	.42
18	740914	18 54.58	38 25.75	112 44.93	9.91	1.42	.76
19	740914	113 48.45	38 4.95	112 47.97	10.00	2.23	.14
20	740914	1843 31.76	38 47.44	112 49.81	5.006	1.87	1.05
21	740915	1747 57.16	38 27.16	113 1.76	25.58	1.08	.07
22	740915	1824 13.50	38 14.60	113 10.58	5.006	2.43	.00
23	740915	2039 48.40	38 40.36	112 49.68	5.006	1.36	.00
24	740916	1523 9.99	38 39.06	112 58.89	.71	1.14	.28
25	740916	2252 28.96	38 31.11	112 50.95	5.006	1.21	.65
26	740916	2349 14.80	38 29.20	113 1.54	5.006	1.37	.37
27	740917	2006 11.41	38 47.42	112 36.79	10.00	1.95	.37
28	740919	1937 3.76	38 38.06	112 42.29	5.006	1.28	.27
29	740920	1454 39.46	38 35.15	112 16.66	10.00	2.27	.13
30	740920	2340 57.84	38 27.29	113 5.44	5.006	1.42	.27
31	740922	1012 58.51	38 6.92	112 53.50	5.006	1.69	.14
32	740923	1309 34.86	38 37.64	112 39.81	5.006	1.76	.29
33	740923	2004 50.95	38 27.77	113 7.05	8.37	1.59	.25
34	740924	14 20.54	38 30.62	113 7.74	14.50	1.71	.22
35	750611	2158 25.81	38 38.37	113 4.33	21.13	1.88	.00
36	750612	2044 41.32	38 44.30	112 48.49	12.94	2.18	.06
37	750612	2258 36.97	38 35.17	112 38.57	8.06	1.44	.17
38	750613	255 54.89	38 38.95	113 17.24	18.06	2.29	.24
39	750613	350 59.06	38 37.09	112 34.96	4.78	.77	.03
40	750613	824 48.20	38 46.34	112 46.20	5.006	1.95	.09
41	750613	827 36.36	38 17.52	112 39.59	5.006	1.31	.11
42	750613	1744 43.93	38 45.32	112 50.50	5.006	2.24	.13

43	750613	2034	59.45	38	36.31	112	36.59	.39	1.40	.08
44	750613	2156	26.62	38	34.82	113	.41	5.006	2.30	.00
45	750614	343	11.25	38	38.83	112	31.88	5.006	.91	.00
46	750614	457	7.46	38	37.67	112	30.47	1.02	1.13	.14
47	750614	559	39.97	38	40.72	112	32.20	5.006	.93	.12
48	750614	743	57.97	38	43.02	112	28.67	1.82	.59	.51
49	750614	1031	32.00	38	36.25	112	34.35	5.006	1.95	.09
50	750614	1034	43.80	38	39.15	112	32.07	5.006	.76	.00
51	750614	1039	46.48	38	36.68	112	32.41	3.42	.88	.07
52	750614	1116	28.34	38	36.31	112	34.10	2.29	.88	.14
53	750614	1247	49.78	38	37.22	112	34.45	9.58	1.11	.18
54	750614	1446	57.54	38	41.95	112	30.96	.83	.85	.02
55	750614	2214	19.08	38	12.86	112	41.04	5.006	2.50	.31
56	750615	819	18.46	38	13.75	112	38.84	5.006	1.75	.01
57	750615	940	5.19	38	36.64	112	33.05	3.38	1.31	.05
58	750615	944	26.26	38	36.49	112	34.10	5.006	1.92	.04
59	750616	33	53.96	38	45.75	112	31.17	1.65	.31	.10
60	750616	843	47.69	38	40.63	112	33.52	.53	.55	.07
61	750616	1042	49.18	38	40.14	112	32.40	.60	.55	.02
62	750616	1313	50.42	38	38.16	112	33.06	4.48	.91	.00
63	750616	2049	15.74	38	42.32	112	38.46	5.006	2.23	.20
64	750616	2331	38.07	38	30.36	112	31.82	5.99	3.35	.82
65	750617	6	27.04	38	15.53	112	52.57	5.006	1.26	.10
66	750617	324	48.38	38	41.69	112	23.90	5.006	1.70	.09
67	750617	330	4.00	38	44.35	112	28.10	5.006	1.14	.25
68	750617	337	44.27	38	43.44	112	30.17	1.06	1.33	.02
69	750617	439	39.17	38	44.88	112	28.82	4.08	1.03	.26
70	750617	729	31.89	38	16.76	112	41.02	2.57	1.59	.05
71	750617	1339	39.40	38	7.78	112	35.02	1.17	2.06	.07
72	750617	1437	8.27	37	38.14	112	41.95	7.45	2.44	.13
73	750619	1300	42.26	38	25.39	113	7.54	14.33	3.93	.20
74	750619	1320	59.43	38	43.71	112	35.80	5.006	1.47	.16
75	750620	2055	19.40	38	40.35	112	43.06	1.96	2.16	.17
76	750621	825	57.85	38	35.55	112	32.45	5.006	1.32	.13
77	750621	1639	57.44	38	45.34	112	49.53	5.006	1.42	.03
78	750621	2023	6.54	38	38.53	112	34.03	4.32	1.24	.17
79	750621	2156	21.36	38	39.48	113	5.42	5.006	2.10	.08
80	750622	351	45.00	38	37.25	112	37.49	3.43	.96	.08
81	750622	545	14.25	38	39.46	112	33.03	5.006	1.05	.05
82	750622	554	36.85	38	40.66	112	31.75	.46	1.14	.12
83	750622	624	9.26	38	52.28	113	2.76	40.15	3.57	.06
84	750622	811	3.28	38	36.83	112	32.85	5.006	.93	.01
85	750622	1043	17.57	38	37.49	112	33.79	5.006	.76	.00
86	750622	1620	22.28	38	42.62	112	39.68	5.006	1.81	.08
87	750622	1918	10.62	38	44.75	112	40.29	5.006	1.16	.17
88	750622	1934	44.11	38	27.62	112	26.62	5.006	1.52	.07
89	750623	655	32.50	38	37.63	112	36.10	1.20	.73	.01
90	750623	1645	31.48	38	37.93	112	27.53	2.14	.82	.07
91	750623	1817	23.56	38	35.64	112	34.15	3.16	1.17	.10
92	750624	29	4.94	38	39.22	112	38.46	5.006	1.59	.58
93	750625	409	10.23	38	39.22	112	34.45	9.15	1.12	.29
94	750625	758	1.65	38	43.33	112	25.92	5.006	1.85	.19

95	750625	1938	28.64	38	50.31	112	28.16	5.00δ	1.70	.94
96	750625	2313	57.50	38	40.60	112	58.92	5.00δ	2.25	.09
97	750626	1210	15.11	38	38.77	112	33.04	.30	.85	.02
98	750626	1230	44.88	38	30.08	113	.04	16.57	4.19	.15
99	750627	141	20.84	38	36.04	112	33.46	5.00δ	.51	.12
100	750628	158	32.45	38	41.17	112	32.62	6.64	.97	.05
101	750628	948	20.79	38	36.03	113	.43	8.42	3.19	.23
102	750628	1603	52.94	38	36.32	112	32.89	5.00δ	1.34	.23
103	750629	213	15.39	38	19.78	112	18.19	5.90	1.29	.13
104	750629	1246	6.75	38	41.65	112	31.22	8.57	.96	.03
105	750629	1445	44.77	38	39.11	112	34.61	.40	.74	.25
106	750630	417	22.24	38	36.15	112	33.35	4.75	1.43	.13
107	750630	425	39.73	38	36.08	112	33.29	3.02	1.68	.13
108	750630	429	20.70	38	35.81	112	33.28	1.70	.75	.15
109	750630	429	42.45	38	36.29	112	33.24	2.90	1.16	.12
110	750630	431	43.99	38	36.08	112	33.60	4.70	1.25	.14
111	750630	436	18.31	38	36.05	112	33.46	4.79	1.39	.14
112	750630	646	48.67	38	36.05	112	33.59	2.72	.75	.07
113	750630	1948	24.85	38	15.77	112	37.79	5.00δ	2.02	.11
114	750630	2211	6.45	38	42.63	112	33.11	6.55	1.22	.11
115	750701	36	16.76	38	35.51	112	33.58	5.00δ	1.40	.23
116	750701	515	44.60	38	35.48	112	31.10	1.73	.56	.25
117	750701	921	36.42	38	41.28	112	29.98	11.07	1.05	.05
118	750701	1717	46.45	38	36.00	112	32.83	3.63	1.20	.12
119	750701	1720	16.20	38	36.28	112	33.42	5.00δ	1.51	.13
120	750702	115	59.92	38	34.30	112	36.65	9.66	1.10	.13
121	750702	201	2.04	38	36.15	112	33.46	.06	1.03	.07
122	750702	517	36.96	38	36.65	112	33.88	.53	.79	.11
123	750702	633	14.61	38	26.47	112	16.81	5.71	1.80	.14
124	750703	245	3.03	38	31.98	113	1.45	5.00δ	1.45	.23
125	750703	430	2.13	38	35.71	112	34.41	5.00δ	.41	.15
126	750703	901	39.61	38	36.37	112	33.70	5.00δ	1.17	.11
127	750703	949	9.90	38	40.85	112	30.76	6.02	.63	.11
128	750703	949	22.78	38	38.26	112	30.14	2.92	.43	.13
129	750703	949	47.12	38	35.50	112	36.13	5.57	.78	.06
130	750703	1016	55.54	38	33.26	112	40.01	5.00δ	.13	.04
131	750703	1305	49.98	38	38.99	112	33.46	.21	.61	.20
132	750703	2046	19.13	39	4.96	112	32.12	5.00δ	2.08	.13
133	750704	404	34.04	38	36.29	112	32.97	.38	.97	.06
134	750704	650	1.90	38	38.52	112	36.56	8.12	.39	.01
135	750704	803	31.03	38	36.45	112	33.73	1.69	1.33	.07
136	750704	1110	40.07	38	36.48	112	33.63	1.00	.79	.06
137	750704	1124	27.72	38	37.80	112	36.29	3.49	.83	.05
138	750704	1250	31.71	38	41.29	112	31.49	7.55	.40	.12
139	750704	1303	20.61	38	28.76	112	33.95	5.00δ	1.03	.08
140	750704	1336	37.32	38	36.34	112	33.61	2.73	1.17	.07
141	750704	2202	43.38	38	41.96	112	33.04	5.00δ	.72	.07
142	750705	458	49.96	38	36.29	112	32.95	4.44	.25	.05
143	750705	812	52.67	38	41.37	112	33.02	5.46	.61	.07
144	750705	2107	3.53	39	21.85	112	45.16	.69	2.16	.32
145	750706	106	12.61	38	36.29	112	33.84	3.96	1.89	.08
146	750706	107	40.81	38	36.21	112	33.71	3.43	1.11	.09

147	750706	246	29.34	38	36.34	112	34.22	3.89	1.02	.09
148	750706	304	18.09	38	36.29	112	33.46	5.008	.63	.00
149	750706	617	4.46	38	42.29	112	32.51	5.008	.76	.05
150	750706	1332	42.85	38	36.18	112	38.95	3.82	.82	.00
151	750706	1621	41.84	38	44.65	112	33.86	6.72	1.06	.05
152	750706	1639	16.10	38	42.34	112	32.38	8.01	1.74	.09
153	750707	110	19.82	38	36.72	112	34.50	5.008	1.18	.18
154	750707	150	33.52	38	36.07	112	33.03	5.008	.71	.14
155	750707	256	36.21	38	28.84	112	19.85	1.13	1.06	.08
156	750707	422	33.39	38	36.08	112	32.84	5.008	.68	.11
157	750707	947	37.32	38	44.58	112	30.54	6.28	1.27	.12
158	750707	1114	51.80	38	37.46	112	35.28	6.43	.79	.12
159	750707	2323	28.73	38	38.42	112	26.01	5.008	1.41	.04
160	750708	337	29.98	38	41.80	112	34.12	5.008	.70	.00
161	750708	356	4.27	38	35.98	112	33.46	2.50	1.14	.11
162	750708	1545	15.02	38	35.90	112	33.56	5.63	1.38	.07
163	750708	1730	.09	38	35.59	112	35.63	4.15	.88	.01

APPENDIX B

STATION LOCATIONS

STATION	LONGITUDE	LATITUDE	ELEVATION (m)
Antelope Valley (ANT)	112°38.36'	38°39.12'	1871.9
Beaver Lake Mountains (BVR)	113°04.66'	38°31.89'	1658.5
Cinder Crater (CIN)	112°38.27'	38°34.39'	1973.2
Dog Valley (DOG)	112°33.36'	38°38.43'	1964.0
Dry Wash (DRY)	112°28.06'	38°45.16'	1707.8
Lincoln Gulch (LIN)	112°52.22'	38°16.57'	2098.2
Lincoln II (LI2)	112°51.62'	38°16.59'	2147.0
Mine (MIN)	112°41.27'	38°29.75'	2055.5
Mud Springs (MUD)	112°24.58'	38°32.08'	2214.1
Mary's Nipple (NIP)	112°25.69'	38°40.95'	2217.1
North Mineral (NOM)	112°49.71'	38°37.91'	1762.7
North Mineral II (NM2)	112°50.23'	38°37.64'	1834.0
Pole Canyon (POL)	112°32.54'	38°25.03'	2409.3
Ranch Canyon (RAN)	112°50.85'	38°25.65'	1982.3
Sandstone (SND)	112°31.72'	38°40.75'	1970.1
Sevier Lake (LAK)	113°02.44'	38°52.90'	1590.0
Sulphur Creek (SLF)	112°33.85'	38°32.69'	2098.2
Thermo (TMO)	113°17.62'	38°15.27'	1590.0
Twin Peaks (TWN)	112°44.35'	38°46.89'	1622.5
Twin Peaks II (TW2)	112°44.63'	38°44.96'	1616.4

APPENDIX C

EARTHQUAKES USED TO COMPILE COMPOSITE FAULT PLANE SOLUTIONS

Composite Fault Plane Solution 1

EVENT	DATE	DEPTH (km)	RMS (sec)
47	06 14 75	5.00	0.12
100	06 28 75	6.64	0.05
114	06 30 75	6.55	0.11
117	07 01 75	11.07	0.05
141	07 04 75	5.00	0.07
143	07 05 75	5.46	0.07
151	07 06 75	6.72	0.05
152	07 06 75	6.72	0.09

Composite Fault Plane Solution 2

EVENT	DATE	DEPTH (km)	RMS (sec)
106	06 30 75	4.75	0.13
109	06 30 75	2.90	0.12
110	06 30 75	4.70	0.14
112	06 30 75	2.72	0.07
115	07 01 75	5.00	0.23
118	07 01 75	3.63	0.12
119	07 01 75	5.01	0.13
120	07 02 75	9.66	0.13

Composite Fault Plane Solution 3

EVENT	DATE	DEPTH (km)	RMS (sec)
37	06 12 75	8.06	0.17
43	06 13 75	0.39	0.08
58	06 15 75	5.00	0.04
80	06 22 75	3.43	0.08
120	07 02 75	9.66	0.13
129	07 03 75	5.57	0.06
163	07 08 75	4.15	0.01

APPENDIX D

PERIODS OF STATION OCCUPATION

STATION	PERIOD OF OPERATION
ANT	June 12, 1975 to June 19, 1975
	June 20, 1975 to July 8, 1975
BVR	Sept 5, 1974 to Sept 24, 1974
	June 11, 1975 to June 12, 1975
	June 13, 1975 to June 14, 1975
	June 15, 1975 to June 19, 1975
	June 20, 1975 to June 22, 1975
	June 28, 1975 to June 29, 1975
	June 30, 1975 to July 2, 1975
CIN	July 2, 1975 to July 8, 1975
DOG	June 12, 1975 to June 19, 1975
	June 21, 1975 to June 23, 1975
	June 24, 1975 to June 30, 1975
	July 1, 1975 to July 8, 1975
DRY	June 22, 1975 to July 8, 1975
LIN	June 12, 1975 to June 14, 1975
LI2	June 14, 1975 to June 19, 1975
MIN	Sept 6, 1975 to Sept 24, 1975
	June 11, 1975 to June 19, 1975
	June 21, 1975 to July 8, 1975
MUD	June 25, 1975 to June 26, 1975
	June 27, 1975 to June 28, 1975
	June 29, 1975 to July 8, 1975
NIP	June 26, 1975 to July 8, 1975
NOM	Sept 11, 1974 to Sept 24, 1974
	June 11, 1975 to June 19, 1975
	June 20, 1975 to July 8, 1975
NM2	Sept 4, 1974 to Sept 11, 1974

POL	July 4, 1975 to July 8, 1975
RAN	Sept 4, 1974 to Sept 8, 1974 Sept 10, 1974 to Sept 11, 1974 Sept 13, 1974 to Sept 24, 1974 June 11, 1975 to June 19, 1975 June 20, 1975 to July 8, 1975
SND	June 28, 1975 to July 8, 1975
LAK	Sept 5, 1974 to Sept 10, 1974 Sept 16, 1974 to Sept 24, 1974
SLF	June 29, 1975 to July 8, 1975
TMO	Sept 5, 1974 to Sept 24, 1974
TWN	June 11, 1975 to June 19, 1975
TW2	June 20, 1975 to July 8, 1975

EPICENTER MAP AND GENERAL GEOLOGY OF THE ROOSEVELT HOT SPRINGS AREA

PLATE I

GEOLOGY FROM HINTZE (1963) AND PETERSEN (1975)

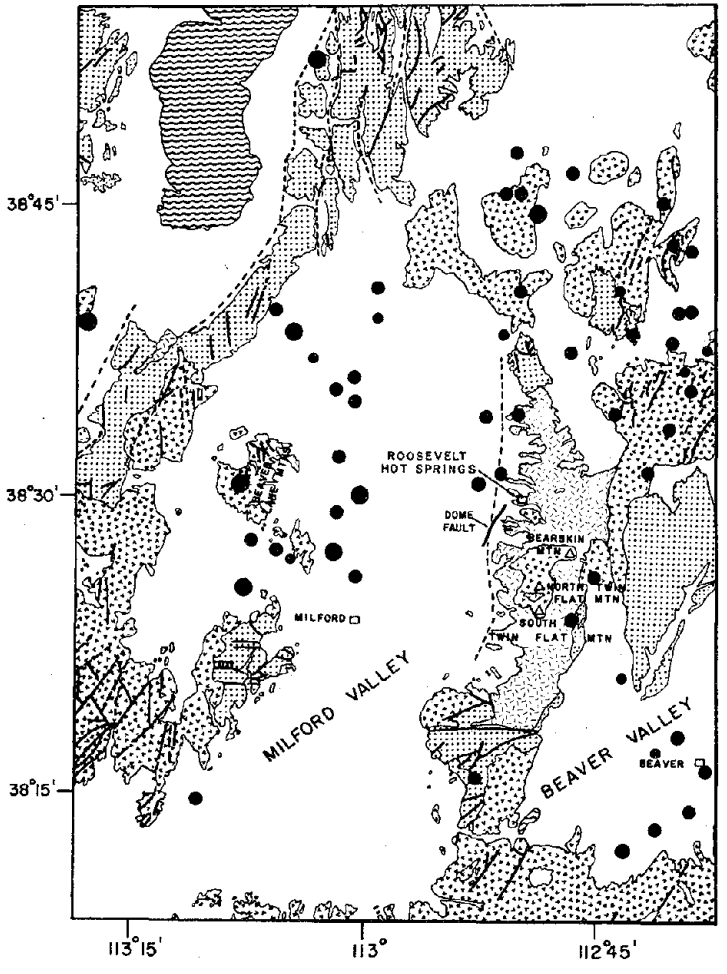

LEGEND

- GRANITE
- ALLUVIUM
- SEDIMENTARY
- VOLCANIC ROCK
- MAPPED FAULT
- ---- INFERRED FAULT
- • FOCAL DEPTH LESS THAN 5 KM.
- • FOCAL DEPTH BETWEEN 5 KM. & 10 KM.
- • FOCAL DEPTH GREATER THAN 10 KM.

SCALE 1:250,000

5 0 5 10 MILES

5 0 5 10 KILOMETERS

PLATE 2

EPICENTER MAP AND GENERAL GEOLOGY OF THE COVE FORT-SULPHURDALE AREA

GEOLOGY FROM HINTZE (1963)

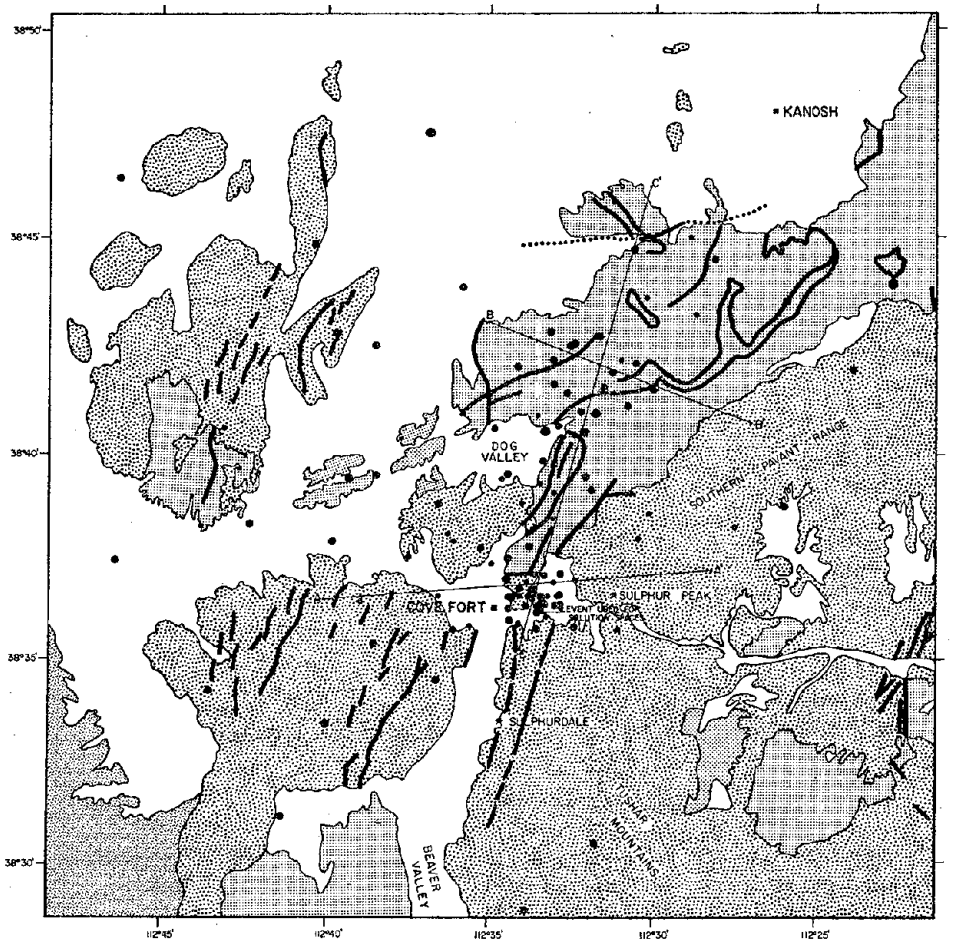

LEGEND

- GRANITE
- ALLUVIUM
- SEDIMENTARY
- VOLCANIC ROCK
- MAPPED FAULT
- INFERRED FAULT
- FOCAL DEPTH LESS THAN 5KM.
- FOCAL DEPTH BETWEEN 5KM. & 10KM.
- FOCAL DEPTH GREATER THAN 10KM.

SCALE 1:62500

1 0 1 2 3 4 MILES

1 0 1 2 3 4 5 KILOMETERS